Spring 5-10-2024

BIO-BASED RIGID POLYURETHANE FOAMS USING MODIFIED HEMP SEED OIL COMBINED WITH FLAME RETARDANTS

Sagar Jariwala
Pittsburg State University, sjariwala@gus.pittstate.edu

BIO-BASED RIGID POLYURETHANE FOAMS USING MODIFIED HEMP SEED OIL COMBINED WITH FLAME RETARDANTS

A Thesis Submitted to the Graduate School
in Partial Fulfillment of the Requirements
For the Degree of
Master of Science

Sagar Jayantibhai Jariwala

Pittsburg State University

Pittsburg, Kansas

May, 2024

BIO-BASED RIGID POLYURETHANE FOAMS USING MODIFIED HEMP SEED OIL COMBINED WITH FLAME RETARDANTS

Sagar Jayantibhai Jariwala

APPROVED:

Thesis Advisor _____
Dr. Ram Gupta, Department of Chemistry

Committee Member _____
Dr. Khamis Siam, Department of Chemistry

Committee Member _____
Dr. John Franklin, Department of English and Modern Languages

ACKNOWLEDGMENTS

I express my deepest gratitude to my research adviser, Dr. Ram K. Gupta, for his outstanding assistance and guidance. His instructional approaches effectively assisted my research activities and encouraged me to achieve creativity and effortlessness. Furthermore, I would like to extend my gratitude for his guidance and unwavering support in exploring and studying novel scientific breakthroughs beyond the confines of my research focus. It enhanced my understanding of recent scientific discoveries, and despite the difficulties, the past two years have been the most fruitful period of my life.

I want to use this opportunity to express my appreciation to Dr. Jeanne Norton, Dr. Jody Neef, Dr. Petar Dvornic, and Mr. Paul Herring, all of whom have played a crucial role in shaping my educational foundation. They have instructed me in the subject matter we discussed in class and offered me guidance and support to enable me to succeed in my present and future studies. I want to express my gratitude to Dr. Khamis Siam and Dr. John Franklin for agreeing to join my thesis committee. In addition, I would like to express my appreciation to the Department of Chemistry and the National Institute for Material Advancement at Pittsburg State University for their kind support for this project.

This thesis work would not have been feasible without the assistance of Yash Desai, Felipe M. de Souza, and Andrew Ouellette. In addition, I express my gratitude to my affectionate friends and colleagues, namely Prasadi Abeysinghe Arachchilage, Magdalene Asare, Arjun Chaudhary, Mansi Ahir, Wang Lin, Vishwa Suthar, Vatsal Chaudhari, and Sahil Chaudhari, who enhance the quality of my journey by making it

more memorable and pleasurable. Their camaraderie, enthusiasm, and joy have consistently brought fresh vibrancy to my existence.

Finally, I want to express my love to my parents, Jayantibhai Jariwala and Rekhaben Jariwala, my grandfather Dahyabhai Jariwala, grandmother Raviben Jariwala, my better half Nishtha Jariwala, and my whole family for their unconditional support and belief despite their distance.

BIO-BASED RIGID POLYURETHANE FOAMS USING MODIFIED HEMP SEED OIL COMBINED WITH FLAME RETARDANTS

An Abstract of the Thesis by
Sagar Jayantibhai Jariwala

In today's world, the idea is to synthesize bio-based polyurethane (PU) goods, which reduces reliance on petroleum-based products. As a result, we produced polyol from hemp seed oil (HSO) and evaluated it using FTIR, GPC, hydroxyl value, and acid value. Hemp seed oil polyol (HSOP) was successfully synthesized and combined with additional ingredients such as catalysts, blowing agents, hardeners, and flame-retardant chemicals to produce stiff polyurethane foams. The focus of this research was to synthesize high-quality flame-retardant rigid polyurethane foams (RPUFs) through the addition of flame retardants. The test results revealed that the HSO-based PU without flame retardants has 47.04 kg/m^3 of apparent density, 92% closed cell content, and a compression strength of 252 kPa.

Regardless of the addition of flame retardants, the shape of the free-rise foams maintained their structure, suggesting that there is acceptable compatibility between the flame retardants and hemp oil-based polyurethane matrix. The physicochemical and mechanical properties, cell morphology, and thermal stability results further confirmed this observation. The majority of the RPUF presented a closed-cell content greater than 92%. Also, a considerable improvement in flame retardancy was observed as the neat HSO-based RPUF had a burning time of 110 seconds and a weight loss of 82%. Yet, the addition of 10 wt% of triethyl phosphate (TEP) reduced to 19 seconds and 5%, respectively. The addition of other two flame retardants, dimethyl methyl phosphate

(DMMP) and expandable graphite (EG), also showed similar trends with flame retardancy and mechanical properties. As a result, our research on the manufacture of biobased RPUFs was successful.

TABLE OF CONTENTS

LIST OF TABLES

LIST OF FIGURES

LIST OF SCHEMES

CHAPTER I

INTRODUCTION

Polymers have played a crucial role in humankind's everyday lives and have helped advance science and technology. Polymers find wide-ranging applications across several sectors, including agriculture, aircraft, automotive, furniture, construction, and packaging [1]. Polyurethane (PU) is one of the most valuable polymers of the time [2]. PU is a versatile polymeric material group with flexible properties that are used in various fields [3,4]. This chapter provides detailed information on the synthesis of PU, different types of PU, their applications, and the factors that might improve the performance of PU.

1.1. Chemistry of Polyurethane

In 1937, while creating competitive polymer alternatives to nylon (polyamide), Professor Otto Bayer and his colleagues developed the first polyurethane [5]. Most polyurethane foams available in the market are produced from non-renewable resources, i.e., petroleum waste [6]. **Figure 1A** illustrates that petrochemically produced polyols and diisocyanates are the primary ingredients used in the commercial manufacture of PU [7,8]. **Figure 2** illustrates the unstable structure of the NCO groups in isocyanate, which accounts for their high reactivity [9]. Carbon is the next element with a lower electron

density than oxygen, which is nitrogen. Nitrogen has an intermediate negative charge, carbon has a positive charge, and oxygen has a negative charge in its intermediate form. During a chemical reaction, the oxygen atom in the hydroxyl group (OH) of the polyol acts as a nucleophile, and it reacts with the carbon atom in the isocyanate, which is an electrophile. This reaction leads to the addition of hydrogen to the NCO group [10]. They must have equal numbers of reacting groups to complete the polyurethane reactions, i.e., isocyanate (NCO) and polyol (OH). In practical processes, an excess of isocyanate is usually used to react with any moisture that may be present. This reaction leads to an unstable carbamic acid-forming, which decomposes into carbon dioxide and amine (**Figure 1B**). In polyurethane foams, the carbon dioxide produced is helpful for cellular structure development and expansion. As seen in **Figure 1C**, the amine might further react with excess isocyanate to create urea [11]. Consequently, the primary polyurethane structure has a urethane linkage and contains other groups, such as ester, aromatic, urea, and ether, in their arrangements [12].

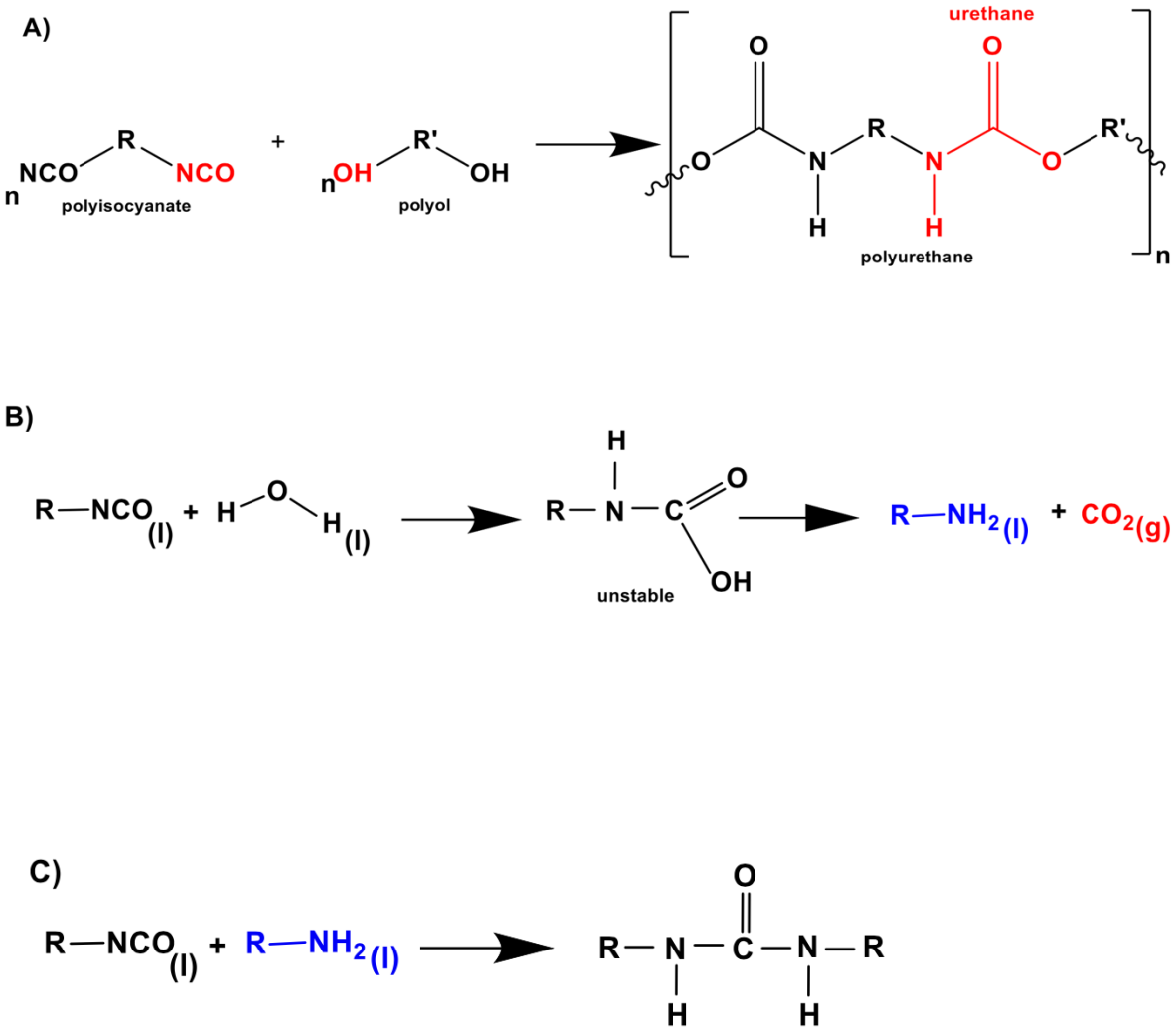

Figure 1. A) Basic chemical reactions between polyol and isocyanate, **B)** Reactions of isocyanate with water, **C)** Reaction of amine with isocyanate. Adapted with permission [12]. Copyright (2010) American Chemical Society.

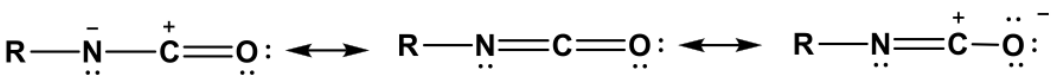

Figure 2. Illustration of the Isocyanate.

1.2 Application of Polyurethane

Since its formation, PU has been considered one of the most essential polymers [13]. PU has been applied to a wide range of products, including foams, adhesives, coatings, sealants, elastomers, and fibers, as shown in **Figure 3** It has also been used in furniture, bedding, cars, packaging, and insulation, among other everyday items. The most common application of PU is foam. The end products of PU foam have a higher force absorption, are thermally acoustic, and have lower density due to the enormous gas phase in the foam. PU foams are classified into two categories: Rigid polyurethane foams (RPUFs) and flexible polyurethane foams (FPUFs). About 38% of PU foam is manufactured as FPUFs, taking the largest portion of the market size [14]. It is used in car seats, interior design, medical equipment, and mattresses [15]. RPUF is the second most popular foam, with 25% of the market size. Due to the excellent mechanical, physical, and thermal insulating properties of the foams, they are used in construction, aerospace industries, automotive, packaging, and transportation [16].

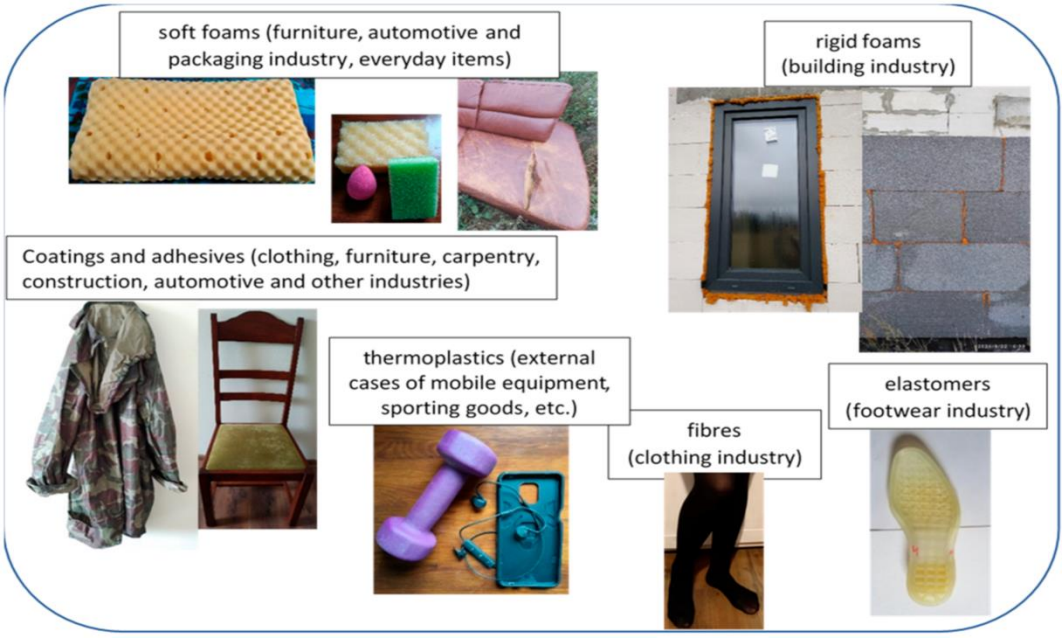

Figure 3. Versatile applications of polyurethanes. Reproduced with permission [17].

1.3 Renewable Sources for Polyurethanes

Most polyurethane foams available in the market come from non-renewable resources, specifically petroleum waste [18]. The primary components used in commercial PU products are typically petrochemically produced polyols and diisocyanates. Scientists and chemists focus on using more environmentally friendly and secure raw materials to limit petroleum consumption [19]. Utilizing renewable resources to prepare polymers is essential for science and the economy. Bio-polyols derived from waste materials or plant oils can successfully substitute petrochemical polyols when producing PU foams [20]. Vegetable oils like canola, sunflower, hemp seed, soybean, and wood are sources of biobased polyol. Using vegetable oil instead of

petroleum oil during the PU production process is one of the appropriate strategies [21]. Vegetable oils have been a tempting substitute because of their unsaturated double bonds and hydroxyl groups, which can be functionalized or used directly to create PU foams. They are also affordable, accessible, and environmentally friendly. **Figure 4** shows that the lipids have been investigated as a source of polyester polyols [22]. While lignocellulose has been studied to produce aromatic polyols, polysaccharides have been used to make polyether polyols.

Figure 4. Bio-based polyols and their renewable sources. Reproduced with permission [22]. Copyright (2021) American Chemical Society.

1.4 Why Hemp Seed Oil?

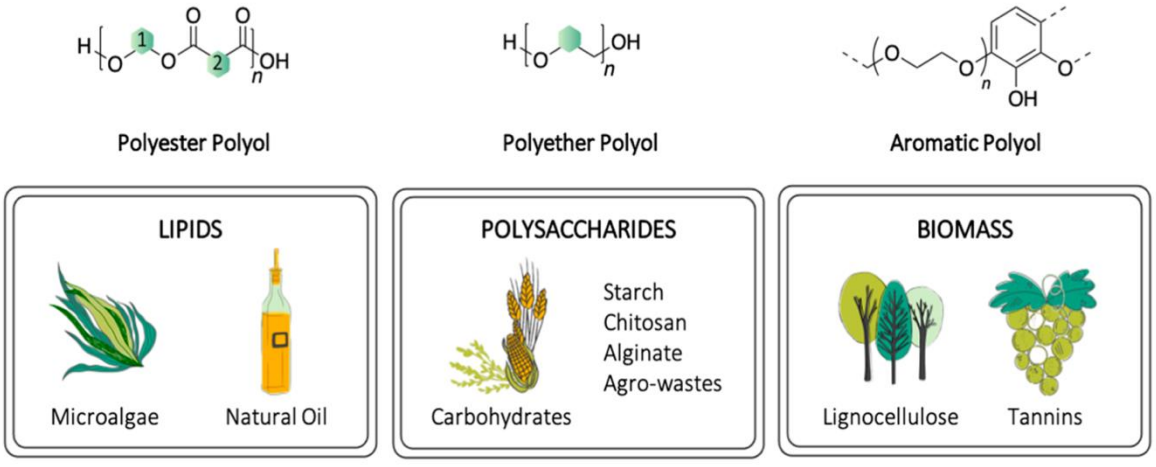

Cannabis sativa L is frequently called hemp, an herbaceous plant used for food, oil, and fiber. Hemp seed oil (HSO) is known for its high oil yield, ranging from 28% to 35%, depending on the region where it is grown [23]. HSO is obtained by cold-pressing hemp seed. Additionally, HSO has been demonstrated to lower blood

pressure and cholesterol and protect against cancer and heart disease [24]. HSO has been positioned as a precious commodity suitable for use in the food, pharmaceutical, nutraceutical, and cosmetic industries due to the distinctiveness of its composition. HSO is distinguished by having a high concentration of n-6 linoleic and n-3 linolenic fatty acids [25]. Its high unsaturation concentration allows various chemical structure changes, including epoxidation, acrylation, hydroxylation, and maleinization [26]. Epoxidized hemp seed oil (EHSO) is currently under investigation as an initial substance for the production of bio-derived epoxy resins used in the manufacturing of plastic, paper, and wood products [27]. Additionally, there have been no reports about the production of rigid polyurethane foams (RPUFs) that incorporate HSO-based bio-polyols and flame-retardants. Despite their versatility, RPUFs are highly combustible. Therefore, it is crucial to enhance their flame resistance to minimize potentially hazardous fire situations that threaten people's lives. Hence, our current research investigates the synthesis of RPUF by using HSO converted into a polyol as a starting material, as seen in **Figure 1**. The transformation of HSO into an HSO-polyol involves an epoxidation reaction followed by ring-opening. It is crucial to note that using HSO as a raw material to create PU with competitive qualities can offer a sustainable method of consuming a potential environmental risk. This would be beneficial for industrial-scale mass production.

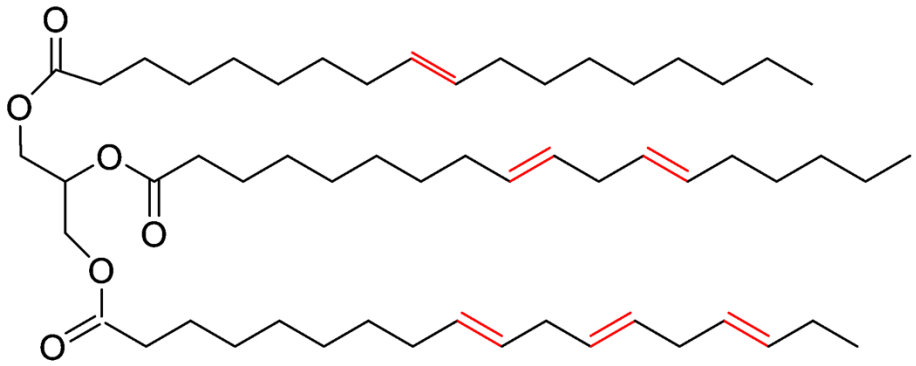

Figure 5. Structure of hemp seed oil.

1.5 Flame Retardants of Polyurethane Foams

Owing to the porous structure of the rigid polyurethane foams, weak covalent connections between bonds such as oxygen, carbon, and hydrogen, and high concentrations of soft segments in the PU, the foams are inherently flambe and speed fire quickly. Moreover, burning RPUF produces a significant amount of smoke that contains CO_2, as well as dangerous gases like CO, NO_x, HCN, and volatile hydrocarbons like toluene, xylene, benzene, biphenyl, and naphthalene, which are harmful to the environment [28]. Therefore, the incorporation of flame retardant (FR) into the RPUF matrix is necessary. The US National Fire Protection Association (NFPA) has released new statistics showing the country's home fire rate has declined. Additionally, these data demonstrated a clear link between the effect of PU foams containing FRs on human safety and their inclusion [29]. FRs may restrict the spread of fire by interfering chemically or physically. **Figure 6** illustrates commonly used flame

retardants in PU foams. Halogen-containing compounds are conventional FRs for RPUF since they can drastically reduce RPUF's flammability. Nevertheless, burning RPUF that contains halogens releases poisonous fumes and corrosive byproducts that are bad for the environment [30]. As a result, halogen-free FRs [phosphorus (P)-based compounds, nitrogen (N)-based compounds, carbon (C)-based compounds, and mineral-like substances have been the subject of extensive research [28].

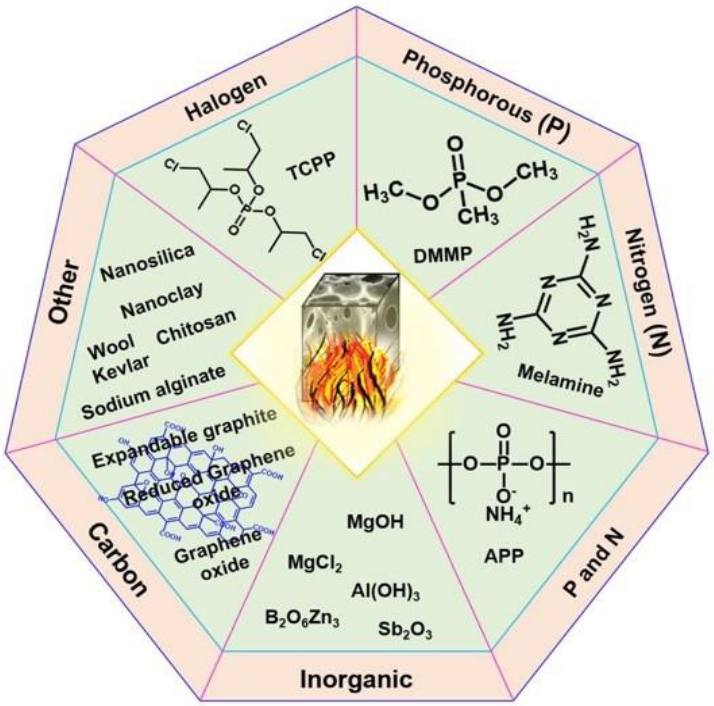

Figure 6. Commonly used flame-retardant used in RPUFs. Adapted with permission [28]. Copyright (2022), American Chemical Society.

There are several mechanisms by which flame retardants can suppress flame propagation. Certain fire retardants create a protective layer, or thermal shield, on the material that serves as a wall between the material and the flame. This layer can absorb

heat, preventing the material from burning or igniting. Thermal shielding is the term for this mechanism. When a material is exposed to high temperatures, gases that suppress flames are released, known as the gas-phase inhibition mechanism [30]. These gases could inhibit combustion, slow down, or stop fires from spreading. **Figure 7** shows that the FRs could absorb heat from the material during heating, causing the material to cool and slowing the combustion process. This process is referred to as the endothermic cooling mechanism. Most FRs typically exhibit the char formation process, which encourages the material's surface to produce a char layer when exposed to high temperatures. In the thermal shielding method, the top char layer is a barrier to keep the underlying material from igniting, just like in the char generation mechanism. FRs occasionally can behave as catalysts to inhibit or stop combustion. FRs achieve this by dissolving the reactive chemicals created during combustion. Moreover, some FRs function by diluting the material's fuel supply, lessening the material's flammability and decreasing the likelihood of it catching fire.

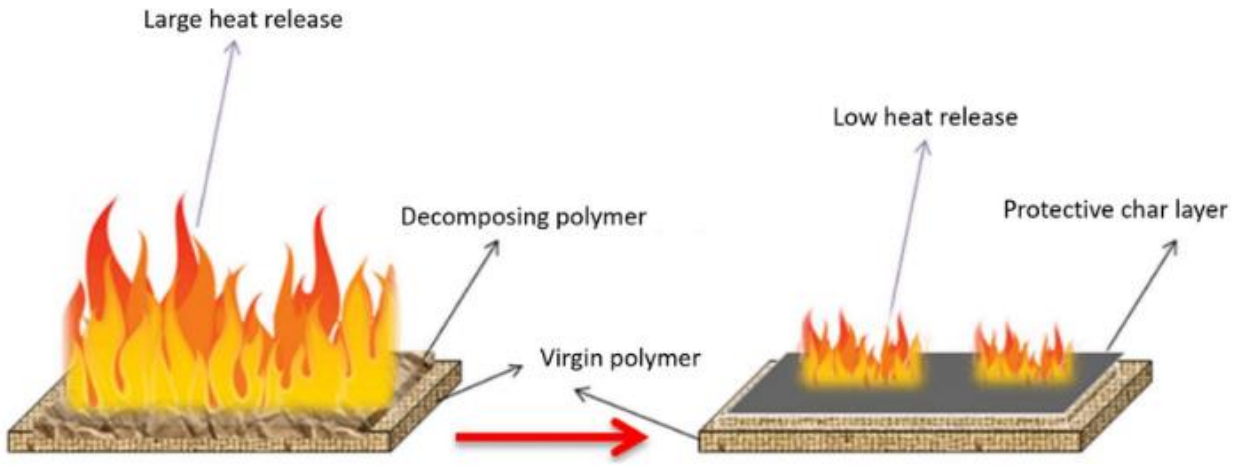

Figure 7. Mechanism of the flame retardants. Reproduced with permission [10]. Copyright (2021) MDPI (This article is an open-access article).

Because of its superior fire-retardant action, P-based compounds have been actively explored as green fire retardants. P-based FRs release radical scavengers for H• and OH• during the gaseous phase of combustion. Furthermore, during burning, they could transform into a thermally stable char layer that can separate the combustible material from the oxygen. As a result, most P-based compounds display gaseous-phase and condensed-phase FR processes. According to earlier research, numerous P-based FRs, such as phosphate ether compounds, phosphorus heterocyclic compounds, and phosphonates, have been used in PU foams. Like this, the condensate and gaseous phases of N-based FRs demonstrate flame-retardant processes. Most derivatives of melamine fall into this group. N-based FRs absorb energy during burning and produce N-containing gases (N_2 and NH_3), which lower oxygen concentrations and other flammable gases in the vicinity [28]. They deposit a charred coating on the top of the burning surface to stop further breakdown. In addition, much attention has been drawn to C-based materials as sustainable green FRs, including carbon nanotubes, expandable graphite, reduced graphene oxide, and graphene. By encouraging the creation of a thick layer of char on the upper burning surface, these kinds of FRs can effectively protect the underlying foam. Among the several FRs that have been reported thus far, dimethyl methylphosphonate (DMMP), triethyl phosphate (TEP), melamine cyanurate (MC), and expandable graphite (EG) were selected as prospective FRs for this investigation due to their excellent fire-retardant activity [31].

The final characteristics of RPUFs depend on the kind of FRs and how they are integrated into the RPUF network. The reactive approach and the additive method are the two common ways FRs are added to the RPUF network. FR is reactively incorporated

into the RPUF matrix during the foaming process by chemically attaching to the FR polymer network. In this instance, the FRs form a permanent link with the polyol, the isocyanate, or both by covalent bonding. By adding FRs, which are not chemically linked to the polymer network, the foam is formed as a distinct component using the additive inclusion approach. However, to connect with the RPUF matrix, FRs create physical interactions with the network, such as hydrogen bonds or van der Waals forces [32]. There are advantages and disadvantages to both reactive and additive incorporation techniques. It frequently delivers better long-term performance and durability because reactive inclusion forms a chemical bond between the FRs and the polymer network. However, it may require more sophisticated processing methods and be more challenging to prepare. Even yet, additive inclusion is more cost-effective and more accessible to employ [33]. However, the FRs may leak over time and lose some of their efficacy. Out of these two approaches, adding additive FR to the RPUF matrix is the most cost-effective and efficient way to produce in large quantities. Thus, using a straightforward additive process, three types of FR with different flame-retardant processes were added to RPUFs in this study. **Figure 8** displays the chemical structures of the FRs.

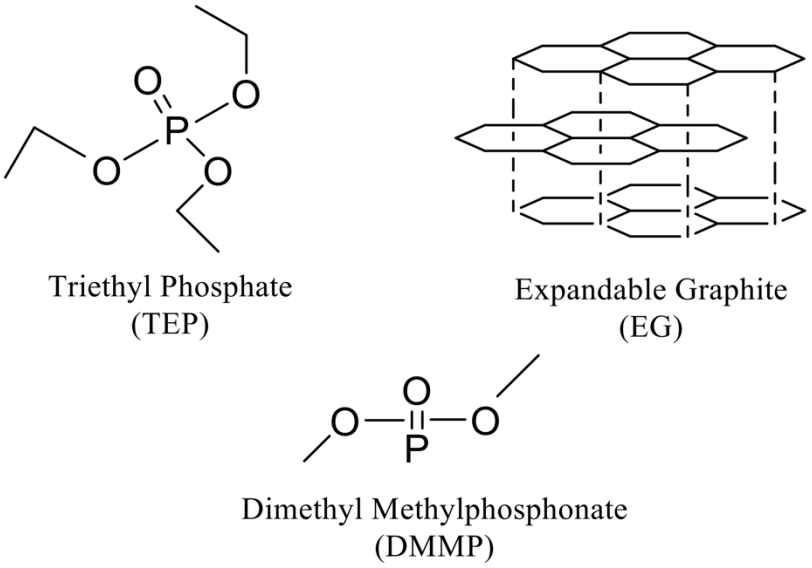

Figure 8. The chemical structure of flame retardants used in this study.

1.6 Objectives of this Thesis

As discussed above, researchers and industry have become more interested in bio-based raw materials for PU manufacture in recent decades because of growing environmental concerns. The objectives of this study were to (i) explore whether highly functional bio-based polyols could be made from hemp seed oil using straightforward wet chemical methods for the production of RPUFs, (ii) lessen the environmental impact of RPUF production by increasing the bio-based content of RPUFs, (iii) reduce the flammability of RPUFs by introducing environmentally friendly FRs, and (iv) evaluate the best compatible FR with a hemp seed oil-based RPUF matrix.

CHAPTER II

MATERIALS AND METHODS

In this study, hemp seed oil (HSO) was used as a starter for polyol synthesis. The transformation process includes (i) Epoxidation of hemp seed oil and (ii) Ring-opening of epoxidized hemp seed oil. The unsaturated fatty acid chains' double bonds are converted into hydroxyl groups. The RPUFs were able to obtain exceptional physicochemical and mechanical qualities by combining a suitable bio-based polyol with a higher hydroxyl number (50/50 weight ratio) with the hemp seed oil-based polyol. A one-shot polyaddition reaction using polyols and isocyanates was used to create HSO-based RPUFs. One pot is used to combine all the essential ingredients for making RPUF, including polyols, isocyanates, catalysts, blowing agents, surfactants, and flame retardants. The most significant feature of this approach is its rapid and incredibly effective mixing. To create a homogenous mixture, all the ingredients except isocyanate were combined first, and then the isocyanate was added. The graphical abstract of this study is displayed in **Figure 9**.

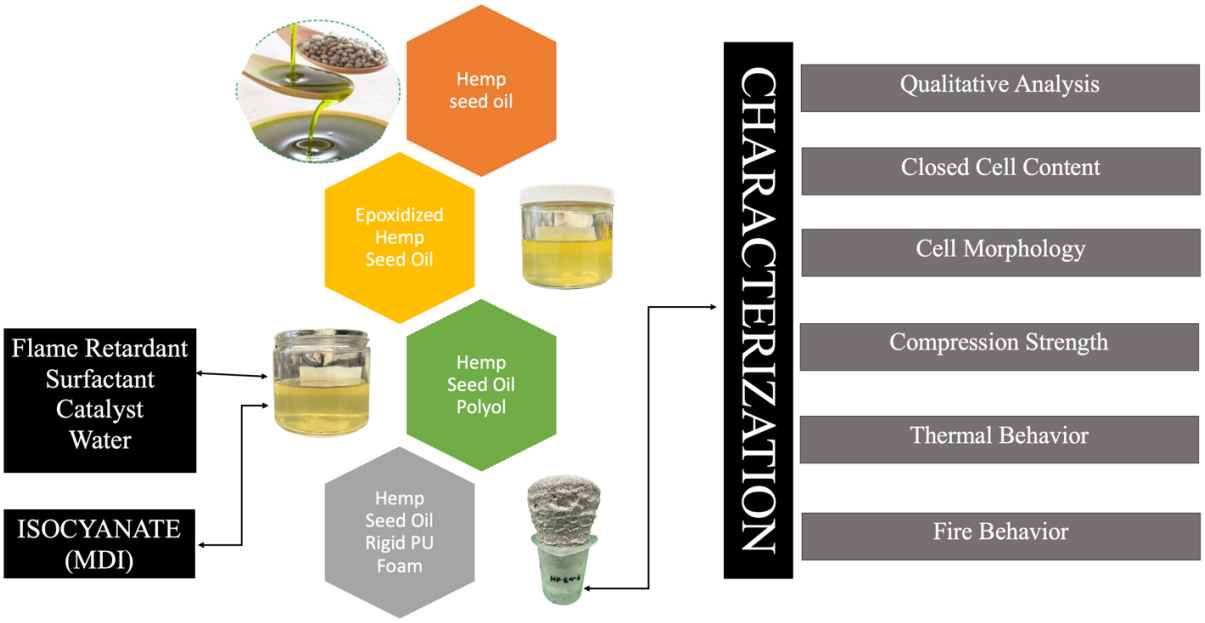

Figure 9. Schematic illustration of synthesis routes and characterization techniques used in this study.

2.1 Starting Materials

Cold-pressed raw Cannabis sativa L. (Hemp seed oil) was a gift. tetrafluoroboric acid, lewitt MP64, sodium sulfate, amberlite IR 120H, sodium chloride, methanol, hydrogen peroxide, acetic acid, and toluene were bought from Fisher Scientific for the manufacture of the HSO-polyol. Dibutyltin dilaurate (DBTDL) and 1,4-diazabicyclo [2.2.2]octane (DABCO) catalysts were acquired from Air products (Allentown, PA, USA) to create the rigid foams. Evonik (Parsippany, NJ, USA) supplied the silicon surfactant (Tegostab B-8404). Jeffol SG-522 and Rubinate M isocyanate (methylene diphenyl diisocyanate) were gifted from Huntsman (The Woodlands, Texas, US). Distilled water was acquired from a nearby Walmart as a blowing agent. The three FRs DMMP, TEP, and EG were obtained from the Sigma-aldrich chemical company.

2.2 Synthesis of Hemp Seed Oil-based Rigid Polyurethane Foam

This reaction procedure was adopted from previously reported literature with some modifications [34][35].

2.2.1 Synthesis of Hemp Seed Oil-based Polyol

First, according to the following method, HSO was epoxidized with peracetic acid formed in situ using glacial acetic acid and H_2O_2 as the reaction carrier. Toluene was used as the solvent, and amberlite IR-120 was used as the solid heterogeneous catalyst. A three-necked round-bottomed flask was filled with 300 g of hemp seed oil, 75 g of amberlite IR -120 resin, and 150 mL of toluene. The reaction setup was equipped by connecting the thermometer, mechanical stirrer, reflux condenser, water bath, and hot plate. The mixture was cooled to 5-10 °C while being stirred continuously. Subsequently, a dropping funnel gradually introduced 33 mL of acetic acid (0.5 mol) and 183 mL of 30 wt.% aqueous H_2O_2 (1.5 mol). The reaction mixture was kept at 5-10 °C by adding acetic acid and H_2O_2, then gradually raised to 70 °C once the addition was complete. The process persisted for 7 hours at this temperature with constant stirring. The reaction mixture was cooled, and the amberlite resin was removed. The reaction mixture was transferred to a separatory funnel and rinsed repeatedly with a 10% sodium chloride solution until the water layer reached a pH of approximately 7. Subsequently, 3 grams of anhydrous Na_2SO_4 were introduced to the isolated organic layer and agitated for 10-15 minutes to eliminate any surplus water in the organic layer. The Na_2SO_4 was filtered, and the organic layer was evaporated and purified using rotary evaporation for 2 hours to eliminate toluene and excess water. Epoxidized hemp seed oil (EHSO) was characterized before the ring-opening process.

The hemp polyol (HSOP) was produced as follows: The mass of methanol was determined based on the 7:1 molar ratio of EHSO and methanol. The catalyst employed was tetrafluoroboric acid (HBF_4) at a concentration of 0.05% of the total weight of the reaction mixture. Methanol and HBF_4 were poured into a round-bottomed flask, and the temperature was gradually raised to 65-70 °C while stirring. EHSO was slowly introduced using a dropping funnel for 40-50 minutes. The reaction mixture was refluxed for 90 minutes after EHSO was completely added. Once the reaction solution reached room temperature, the necessary quantity of Lewatit MP64 resin was introduced and agitated for 45 minutes to catalyze the ring-opening reaction by eliminating excess protons from the system. The molar ratio of Lewatit MP64 to HBF_4 was set at 3:1. The reaction mixture was removed from the resin. Then, rotary evaporation was conducted for 3 hours to eliminate any remaining moisture and unreacted methanol. The hemp oil-based polyol was labeled as HSOP. The alterations in chemical composition during the production of hemp polyol from carbon monoxide were examined using qualitative and quantitative tests.

2.2.2 Synthesis of Flame-Retardant Rigid Polyurethane Foams

The one-pot free-rise method was used to prepare FR-RPUFs. The HSO-based RPUFs were prepared using a one-pot method and formed inside a disposable plastic cup mold, as displayed in **Figure 10**. **Table 1** shows the formulations of rigid polyurethane foams made from hempseed oil. Three foams were created with varying DMMP, TEP, and EG levels. The additives consisted of escalating levels of DMMP, TEP, or EG flame retardants along with 0.18 g of A-1, 0.04 g of T-12, 0.4 g of B8404 surfactant, and 0.8 g

of water. In component A, the HSPO, commercial polyol SG-522 (50/50 wt./wt. ratio), and additives were combined in a disposable plastic cup using a high-speed mechanical stirrer for 1-2 minutes to create a consistent mixture. The weighted isocyanate component B was added to the blended component A, and the mixture was agitated at a speed of 2000-2500 rpm for 20-30 seconds. The mixture was poured into the mold, causing the foam to expand unrestrictedly. The foam was left to cure at room temperature for seven days to finish the polymerization process. An investigation was conducted on how FRs impact the inherent flame resistance of the foams. The RPUFs containing 0 to 10.61 wt.% of all the FRs were created using the same method.

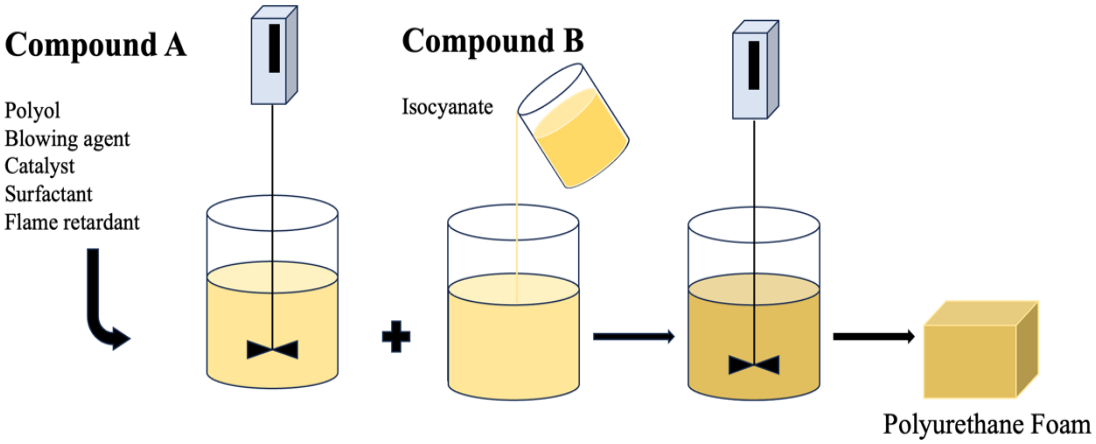

Figure 10. Preparation of hemp seed oil-based rigid polyurethane foams.

Table 1. Formulations of RPUFs. All numbers are in grams (g) except wt.% of FR.

Ingredient	Control (g)	F-1 (g)	F-2 (g)	F-3 (g)	F-4 (g)	F-5 (g)	F-6 (g)
HSOP	10	10	10	10	10	10	10
SG-522	10	10	10	10	10	10	10
A-1	0.18	0.18	0.18	0.18	0.18	0.18	0.18
Water	0.8	0.8	0.8	0.8	0.8	0.8	0.8
T-12	0.04	0.04	0.04	0.04	0.04	0.04	0.04
B-8404	0.4	0.4	0.4	0.4	0.4	0.4	0.4
MDI	29.1	29.1	29.1	29.1	29.1	29.1	29.1
FR (wt.%)	0 (0)	1 (1.94)	2 (3.80)	3 (5.60)	4 (7.33)	5 (9.0)	6 (10.61)

2.3 Characterization

2.3.1 Characterization of Hemp Seed Oil, Epoxidized Polyol, and Polyol

Hemp seed oil obtained from a retailer and hemp oil-based compounds like EHSO and HSOP synthesized in a laboratory were examined and characterized using traditional chemical techniques [34,36].

2.3.1.1 Iodine Value

The oil's iodine value (IV) indicates the unsaturation level. IV is the amount of iodine in grams that can react with double bonds per 100 grams of oil. The study calculated the number of double bonds in the initial hemp seed oil, intermediate EHSO, and final HSOP using the iodine value. The Hanus method (IUPAC 2.205) experimentally estimated the iodine value by placing a precise 0.3 g sample in a 250 mL flask with a glass stopper. 10.0 mL of $CHCl_3$ was added to the flask to dissolve the oil. Next, the Hanus reagent (20.0 mL) was added and gently agitated. The flasks were covered with aluminum foil and stored in a dark room for one hour. Subsequently, 20.0 mL of a 10% potassium iodide solution, 50 mL of HPLC grade water, and six drops of

the starch indicator were added. The mixture was vigorously shaken and diluted with an aqueous sodium thiosulfate (NaS_2O_3) until colorless. The IV was calculated using equation 1, where T represents the normality of the Hanus reagent, V_a is the volume of NaS_2O_3 in the sample, V_b is the volume of NaS_2O_3 in the blank, and W is the weight of the sample. The percentage conversion of double bonds (%C) and theoretical maximum oxirane oxygen content per 100 g of oil were calculated using equations 2 and 3. IV_0 represents the iodine value in HSO, IV_f is the iodine value in HSOP, MM_i is the atomic mass of iodine (126.9 g/mol), and MM_o is the atomic mass of oxygen (16.0 g/mol).

$$IV\left(\frac{gI_2}{100g}\right) = \frac{12.69 \times T \times (V_a - V_b)}{W} \quad (1)$$

$$\%C = \frac{(IV_0 - IV_f)}{IV_0} .100 \quad (2)$$

$$00_{th} = \left\{\frac{IV_0/2MM_i}{100+(IV_o/2MM_i)\,MM_0}\right\} . MM_0 100 \quad (3)$$

2.3.1.2 Epoxol Oxirane Oxygen Content

The oxygen concentration of epoxol-oxirane in an epoxide oil indicates the number of epoxide groups present. This value is shown as a percentage (% EOC). This study used the epoxol-oxirane oxygen (ACS-OXI) approach to quantify the epoxol-oxirane content in EHSO produced from hemp seed oil epoxidation. The procedure for calculating %EOC is as follows: The required sample amount (W = 1.6 / anticipated EOC%) was measured and dissolved in 50.0 mL of TEAB solution in an Erlenmeyer flask. The mixture was titrated with 0.10 N perchloric acid until it changed color from

blue to green, with the assistance of a crystal violet indicator. Equation 4 was utilized to calculate the oxirane content (%EOC). Equation 5 was used to determine the percentage conversion of the epoxidation process, as indicated by the investigation's results.

$$\%EOC = \frac{Titration\ volume \times Normality_{perchloric\ acid} \times 1.6}{Sample\ weight} \quad (4)$$

$$Relative\ fractional\ conversion\ of\ oxirane\ (\%\ ROC) = \frac{00_{exp}}{00_{th}}\ .100 \quad (5)$$

2.3.1.3 Hydroxyl Value

The hydroxyl number of oil/polyols is crucial for determining functionality and reactivity in the production of PU foams. The hydroxyl number was determined by titrating the oil/polyol with a 1.0 N standard solution of sodium hydroxide in the presence of a phenolphthalein indicator, using the phthalic anhydride pyridine (P.A.P) procedure (IUPAC 2.241). A 0.5 g sample was placed in a glass container, followed by the addition of 10.0 mL of hydroxyl reagent (phthalic anhydride solution in pyridine). The sample vials were sealed and placed in a 100 °C oven for 70 minutes, being agitated every 15, 30, and 45 minutes. Subsequently, the samples were cooled to ambient temperature. Subsequently, 10.0 mL of HPLC-grade water and 20.0 mL of isopropanol were combined, followed by the addition of phenolphthalein at a concentration of 10 g/l. 1.0 N NaOH was added to the mixture until the color changed to pink. Equation 6 was used to get the experimental hydroxyl number of HSO, EHSO, and HSOP.

$$Hydroxyl\ number\ \left(\frac{mg\ KOH}{g}\right) = \frac{56.11 \times 1.00 \times (V_0 - V_S)}{W} \quad (6)$$

2.3.1.4 Acid Value

Polyols' acidity directly impacts the quality of the foaming process by potentially interacting with the primary catalyst employed in the RPUF foaming reaction. The acid values of the oils and polyol were determined using the IUPAC 2.201 acid value indicator method. This procedure weighed 3 grams of the sample in a conical flask. The oil was dissolved in a solvent mixture consisting of 30 mL of isopropanol, toluene, and a phenolphthalein indicator. The mixture was titrated with 0.1 N potassium hydroxide until it reached the pink endpoint. The acid value of the samples was determined by applying equation 7, with V being the titration volume and W representing the weight of the sample.

$$Acid\ value\ \frac{mg\ KOH}{g} = \frac{56.11 \times 0.1 \times V}{W} \quad (7)$$

2.3.1.5 Viscosity

The viscosity of the polyol impacts the movement of the blowing agent and other reactants within the polyol matrix. The viscosity of the polyol can significantly affect the creation of polyurethane foam, influencing foam density, cell size, and other factors. The viscosities of HSO and the chemically produced HSOP were determined using an AR 2000 dynamic stress rheometer from TA Instruments, USA. The investigation was conducted at room temperature utilizing linear shear stress and ramp rate ranging from 1 to 2,000 Pa. A cone plate with a 2° angle and 25 mm diameter was used.

2.3.1.6 Fourier Transform Infrared Spectroscopy

The primary goal of Fourier transform infrared (FTIR) spectroscopy is to identify the functional groups present in a chemical molecule. Particular infrared radiation is absorbed, causing a unique peak at a specific wavenumber, determined by the chemical bonds within the functional groups. This study showed changes in the chemical composition of HSO to EHSO and HSOP using FTIR spectroscopy. FTIR spectroscopy was performed via the attenuated total reflection method on a PerkinElmer Spectrum Two Spectrophotometer, as illustrated in **Figure 11.** The spectroscopy was conducted within the 4000−500 cm^{-1} region with a resolution of 4 cm^{-1}.

Figure 11. Digital image of FTIR spectrometer.

2.3.1.7 Gel-Permeation Chromatography

Gel permeation chromatography (GPC) is a technology used to separate polymer molecules in a solution according to their sizes. The sample is typically dissolved in the

mobile phase solvent before being placed onto a permeable column. As the mobile phase fluid flows through the absorbent layer, smaller molecules spend more time in the porous layer, while larger molecules go through faster. Gas phase chromatography (GPC) was performed on HSO, EHSO, and HSOP using a water system at Milford, Massachusetts, USA **(Figure 12)**. The research sought to differentiate each molecule according to its molecular size. The system consisted of a Phenogel 5 μm, LC column of 300 × 7.8 mm, including four different pore sizes: 50, 102, 103, and 104 Å. The mobile phase comprised tetrahydrofuran (THF) flowing at a rate of 1 mL/min and held at a temperature of 30 °C. The 20 mg sample was diluted in 1 mL of THF, and a 20 μL aliquot of the solution was loaded onto the column.

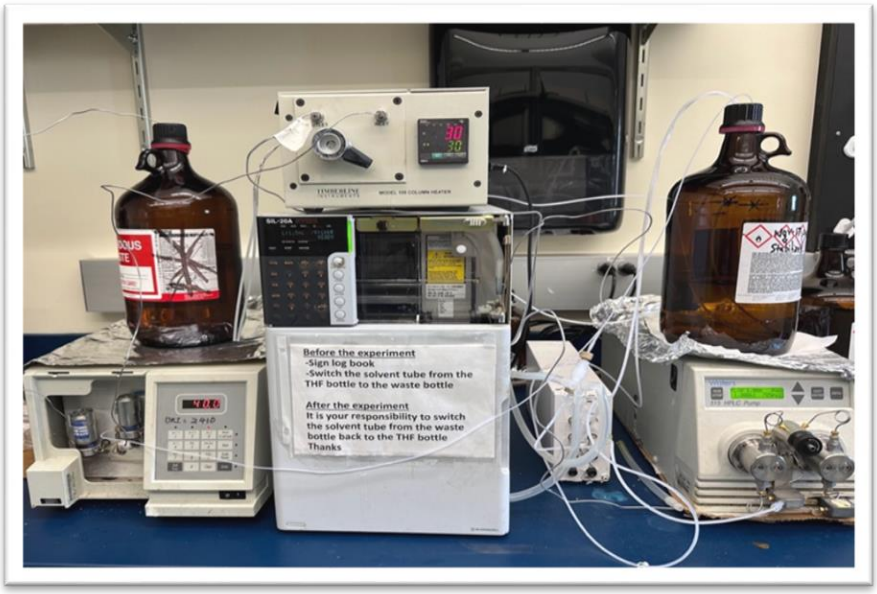

Figure 12. Gel Permeation Chromatography Instrument.

2.3.2 Characterization of HSO-based RPUFs.

The physical, mechanical, and thermal properties of the RPUFs were examined using different experiments such as apparent density measurement, closed cell content

analysis, scanning electron microscope imaging, compressive strength testing, horizontal burning test, and thermogravimetric analysis. Each RPUF was tested for apparent density, closed cell content, and compressive strength using a cylindrical sample measuring approximately 4.6 inches in diameter and 2.5 inches in height. The mean error of each sample was verified through three repeated tests conducted under comparable conditions.

2.3.2.1 Apparent Density

The apparent density of RPUF affects its application due to its correlation with mechanical behavior, morphology, insulation, and other aspects. The foam density was determined following the ASTM D1622 standard (equation 8). The precise measurements of the cylindrical samples were taken at two randomly chosen spots using a Vernier caliper to calculate the geometric volume, and the weight was determined using an analytical balance.

$$Density\ \frac{Kg}{m^3} = \frac{Weight}{Geometric\ volume} \quad (8)$$

Figure 13. Foam sample used for apparent density testing.

2.3.2.2 Closed Cell Content

Closed cell content (CCC) is the proportion of sealed cells inside the cellular arrangement of the RPUF, which indicates the air, moisture permeability, and compressive strength of the material. RPUFs with superior insulating and mechanical qualities typically had a higher proportion of closed cells. An Ultrapycnometer (Ultrafoam 1000) was utilized to measure the quantity of CCC in the RPUFs created in this research. The test method adopted was ASTM D2856 standard procedure **(Figure 14)**.

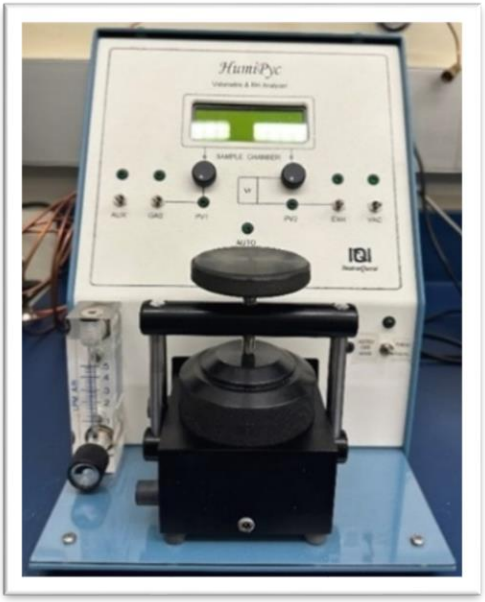

Figure 14. Digital image used to measure CCC instrument.

2.3.2.3 Scanning Electron Microscope (SEM)

SEM is an essential instrument for observing the shape of foam cells. The cellular structure of the RPUFs was examined by analyzing pore shape, pore size, and pore

distribution by SEM images. RPUF samples were sliced into small cubes perpendicular to the growth direction. A thin layer of gold was applied to the top surface using a magnetron sputter from Kurt J. Lesker Company in Jefferson Hills, PA, USA **(Figure 15 left)**. This was done to enhance image quality by preventing charge buildup through conductive coating. The SEM pictures were seen with a Thermo Scientific Phenom instrument set at an accelerating voltage of 5 kV and a magnification of 300 μm **(Figure 15 right)**.

Figure 15. Instrument for using SEM morphology.

2.3.2.4 Compression Strength Test

The mechanical properties of RPUF serve as significant indicators of its compatibility and efficiency. The compressive strength of the RPUFs was tested in the direction of foaming using an Instron Universal Testing Machine **(Figure 16)** controlled by the Blue Hill software following the ISO 844:2016 standard. The movable crosshead

was moved at a speed of 3 cm/min until the compressive stress change achieved a relative deformation of 30%.

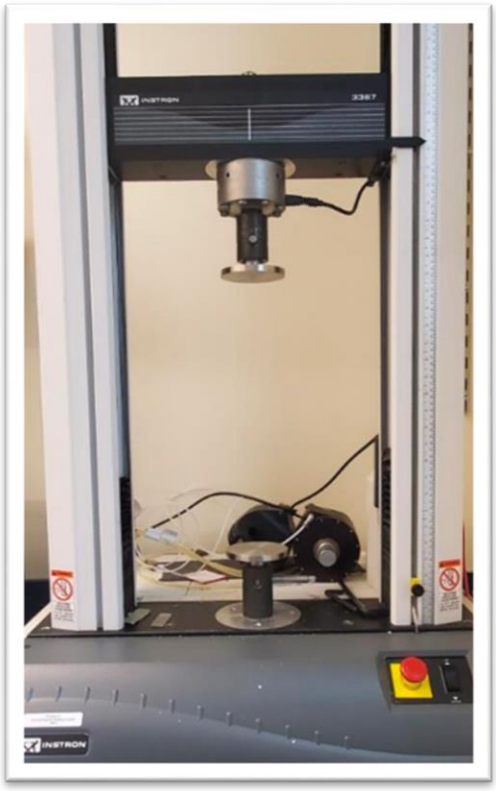

Figure 16. Digital images for universal testing machine.

2.3.2.5 Horizontal Burning Test

The fire performance of the RPUFs was evaluated using the horizontal burning test method as per the ASTM D 4986-18 standard; the foams were laid horizontally in a chamber equipped with a fume hood, as seen in (**Figure 17)**. The sample measured 150 mm in height, 50 mm in length, and 12.5 mm in thickness. During the test, a flame was briefly placed on one end of the object before being withdrawn. Subsequently, the time required for self-extinguishment and the weight reduction percentage were measured.

Figure 17. Chamber for the horizontal burning test.

2.3.2.6 Thermogravimetric Analysis

Thermogravimetric analysis (TGA) gives essential insights into the thermal stability, thermal degradation characteristics, and flame-retardant effectiveness of RPUFs. TGA of RPUFs was performed using a TA Instruments thermogravimetric analyzer (TGA 550) controlled by TRIOS software **(Figure 18)**. The samples' mass loss fluctuation under a nitrogen environment was recorded from 25 to 700 ℃ with a heating rate of 10 °C/min.

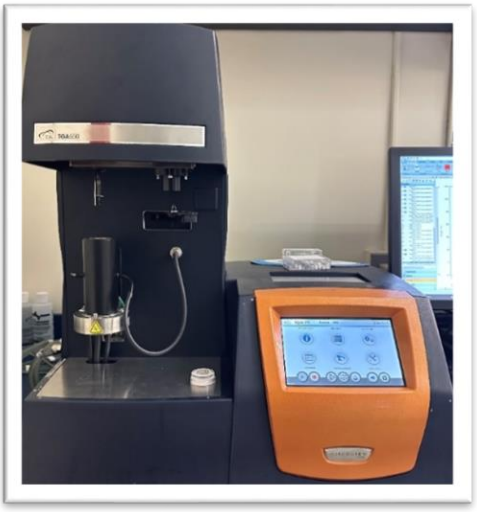

Figure 18. Instrument for thermal analysis.

CHAPTER III

RESULTS AND DISCUSSION

3.1 Characterization of HSO, EHSO, and HSOP

In this study, the double bonds of HSO were converted into epoxy groups by the in-situ formulation of peroxy acid. This research utilized this method to improve the efficacy of HSO. The experiment used an optimized in-house formulation with a molar ratio of 1:0.5:1.5 for C=C, CH_3COOH, and H_2O_2, respectively. Acetic acid was used as the oxygen transporter, and H_2O_2 was used as the oxidation agent. This epoxidation involves reactions occurring in both organic and aqueous phases. Therefore, it is essential to monitor the reaction's temperature closely. The temperature of 70 °C was chosen as the best condition for this study because higher temperatures led to decreased selectivity of double bonds and increased occurrence of side reactions. Based on previous research, extended reaction periods are necessary due to the slow synthesis of peracetic acid. Therefore, the stable and cost-effective ion-exchange resin Amberlite IR-120 was utilized as a catalyst to enhance the reaction rate. Salmi et al. noted that the elevated viscosity and density of vegetable oils can greatly impede mass transfer, decreasing overall reaction speed [37,38].

The ring-opening reaction gives different products depending on the ring-opening reactants. Additionally, water, carboxylic acids, alcohols, hydrogen peroxide, and amines are used as ring-opening agents, whereas the strong acids, Lewis bases, and Lewis acids serve as catalysts. Methanol was utilized as a ring-opening reagent in this work in order to enhance the hydrophobic characteristics of EHSO. The catalyst HBF_4 was used for its ability to produce polyols with a high OH content. **Scheme 1** presents a possible reaction derived from prior research [37][39][36].

The previous discussion characterized the physiochemical characteristics of HSO, EHSO, and HSOP, including iodine value, epoxy-oxirane oxygen content, hydroxyl number, acid value, and viscosity. **Table 2** reports the average test results at ambient temperatures.

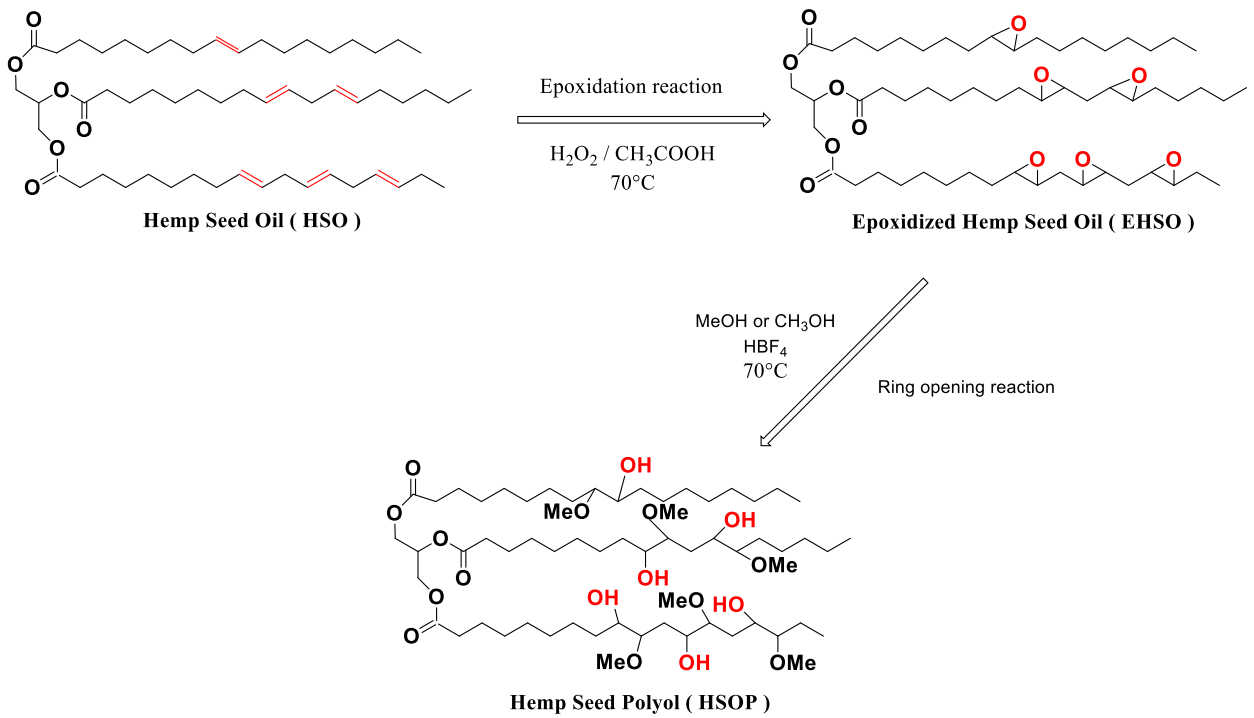

Scheme 1. General reaction scheme for the epoxidation and oxirane ring-opening reaction of ricinoleic triglyceride.

Table 2. Characteristics of HSO, EHSO, and HSOP.

Parameter	Unit	Hemp seed oil (HSO)	Epoxidized hemp seed oil (EHSO)	Hemp seed oil polyol (HSOP)
Iodine value	g I_2/ 100 g	124.31	1.28	0.87
Epoxy-oxirane oxygen content	%	-	5.9	0.1
Hydroxyl number	mg KOH/g		-	209
Acid value	mg KOH/g	12.3	4.7	1.8
Viscosity @ 25 °C	Pa. s	0.02743	0.2618	6.367

As found experimentally, the iodine value of HSO aligned with the expected range from prior literature [25]. The iodine values of EHSO and HSOP indicate a notable reduction in the unsaturation of HSO. The conversion rate of the double bond during epoxidation was around 99.3%. The Fourier Transform Infrared (FTIR) spectra of unmodified HSO that has undergone epoxidation are shown in **Figure 19**. The 3011 cm^{-1} and 1659 cm^{-1} peaks represent the stretching vibrations of =C-H and C=C bonds, respectively. The presence of unsaturated bonds in the molecule in these peaks suggests HSO. The peaks associated with unsaturated bonds were no longer detectable in the EHSO- FTIR spectra. A noticeable peak at 848 cm^{-1} appeared because of the presence of C-O-C in the epoxy oxirane groups. The results show the successful application of our epoxidation reaction method, even with high-viscosity oils [40].

After the oxirane ring-opening process, the hydroxyl number, viscosity, GPC, and FTIR tests were used to confirm the necessary preparation of the HSOP. The hydroxyl number of the produced HSOP was 209.23 mg KOH/g; this amount was used to calculate the quantity of MDI needed to synthesize the rigid polyurethane foams. Prior research has documented bio-based polyols with varying levels of hydroxyl functionality for creating rigid polyurethane foams. Suresh et al. created new bio-based polyols from cardanol with hydroxyl values ranging from 350 to 400 mg KOH/g for rigid polyurethane foams (RPUF). Bote et al. created soybean meal polyols with hydroxyl levels ranging from 550 to 650 mg KOH/g for use in RPUF. synthesized bio-based polyols from sunflower and waste cooking oil with hydroxyl numbers of 180 mg KOH/g and 161 mg KOH/g for rigid polyurethane foam, respectively. Hence, the synthesized HSOP was verified to be appropriate for manufacturing RPUF [35].

The synthesis of polyol was confirmed by FTIR spectroscopy and GPC methods. Following the ring-opening process, the epoxy oxirane ring's peak weakened and disappeared. In contrast, the peak at 3472 cm^{-1} was associated with stretching- OH, as shown in **Figure 19**. This discovery suggests that the epoxidized oil underwent ring-opening, forming additional -OH groups [41].

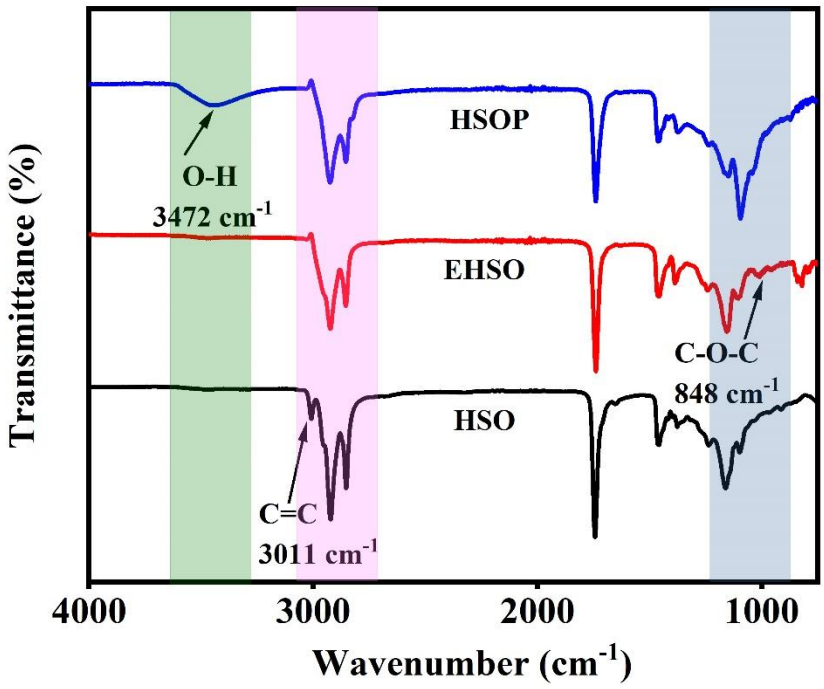

Figure 19. FTIR spectrum of HSO, EHSO, and HSOP.

GPC analyzes individual molecules by sorting them according to their size. Typically, smaller molecules exhibit increased retention time as they traverse the porous column structure and move more slowly through the stationary phase. Additionally, a giant molecule cannot pass through tiny pores and moves fast through the column. **Figure 20** displays HSO, EHSO, and HSOP retention peaks determined by gel permeation chromatography. The HSO chromatogram has a distinct elution peak at 32.4 minutes. In contrast, the EHSO and HSOP chromatograms have a well-defined elution peak at 32.7 minutes and 32.2 minutes. Compared to the HSO chromatogram, the distinctive peak of the HSOP chromatogram exhibited a little leftward shift due to the higher molecular weight [38,42].

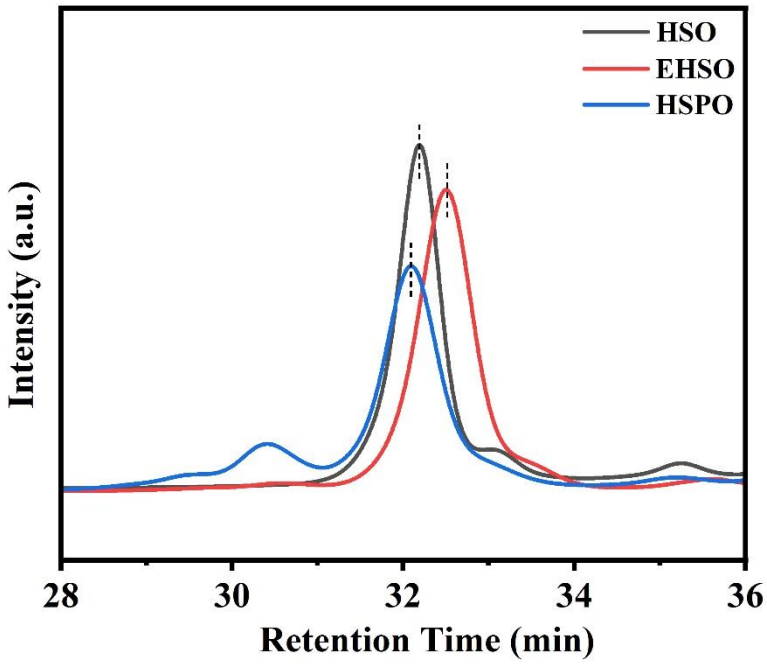

Figure 20. Gel permeation chromatograms of HSO, EHSO, and HSOP.

Viscosity is an important characteristic that indicates molecules' molecular weight and chemical bonding. The synthesis progress was analyzed by the viscosity. The viscosity of polyols is mainly determined by factors such as molecular weight, branching, cross-linking, and the types of functional groups in their chemical structure. As the molecular weight of polyols grows, viscosity typically increases due to the more excellent resistance to the movement of more giant molecules [43]. A strongly branched or cross-linked polymer might elevate viscosity due to limited movement. Functional groups in polyol molecules, such as hydroxyl, carboxylic acid, and amine, can enhance viscosity through chemical interactions [44]. The viscosity of epoxides increased compared to oil and even more in polyols in this investigation. The higher viscosity of HSOP (6.3 Pa.s) is likely a result of the increased molecular weight and the development of numerous additional

hydrogen bonds facilitated by hydroxyl groups. Based on the comprehensive test outcomes, it is clear that both the epoxidation and ring-opening reactions were effective [45]. The percent yield of HSOP after both processes was around 88% and was determined by dividing the final weight of HSOP by the initial weight of HSO.

3.2. Preparation of HSO-based RPUFs

Multiple reactions occur during the one-shot foaming process of RPUFs. The primary reaction involves isocyanate crosslinking with the polyol to generate urethane, then reacting with water to sustain the foaming process. During the foaming reaction, the isocyanate combines with water to produce carbamic acid, which then decomposes into amine and carbon dioxide gas, leading to the formation of the dense foam structure of the RPUFs [46]. Moreover, due to their polarity and density differences, a surfactant must be used to prevent the phase separation of polyol and isocyanate. Tertiary amine-based (JEFCAT) and organotin-based (T-12) catalysts enhanced the reaction rate. **Figure 21** shows the digital images of the prepared HSO-RPUFs, which are labeled as FR-1, FR-2, FR-3, FR-4, FR-5, and FR-6 based on their FR type and quantity. The synthesized RPUFs were then cut into different shapes (cylindrical and strip-shaped) and tested for physiochemical and mechanical properties [47][48].

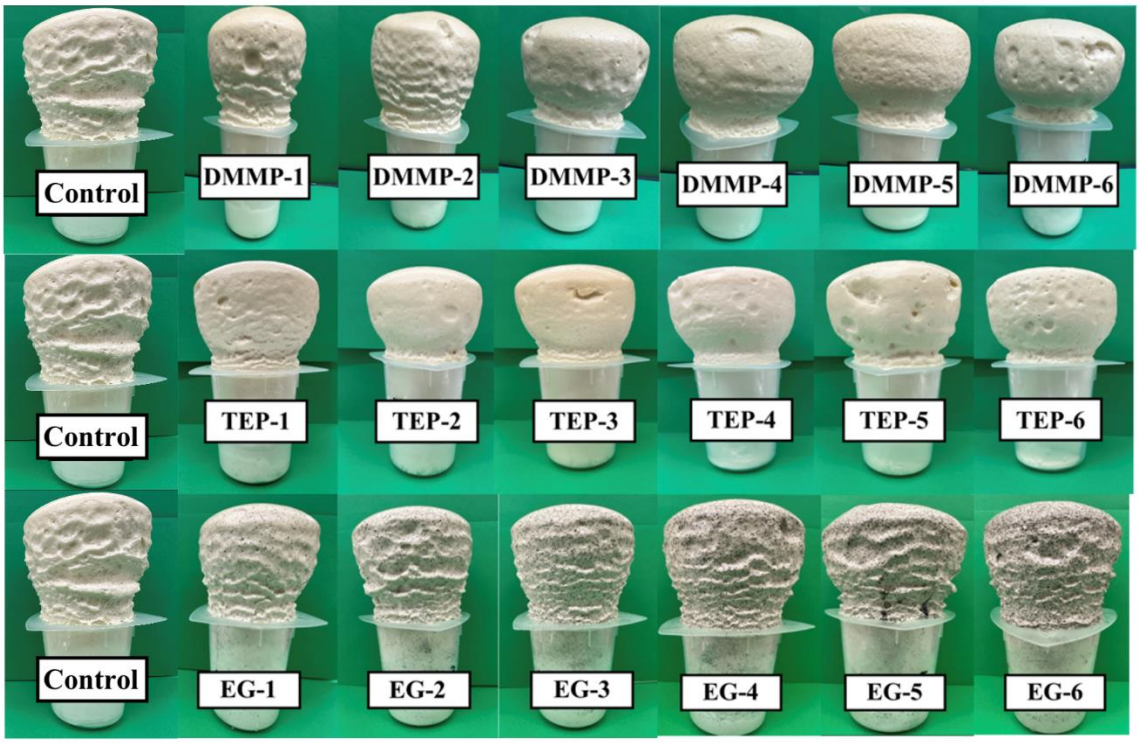

Figure 21. Digital photos of the HSO-RPUFs with different amounts of FRs (A) DMMP, (B) TEP, and (C) EG.

3.3 Characteristics of HSO-RPUFs

3.3.1 Apparent Density

The density of RPUFs considerably affects their surface and mechanical properties. **Figures 22** display the densities of all samples produced with three different types of flame retardants (DMMP, TEP, and EG). The results indicated that the density of RPUFs with various flame retardants was lower than that of pure RPUFs. The control sample of HSO-RPUF had an apparent density of 47.04 kg/m^3, whereas the HSO-RPUF samples containing flame retardants varied in apparent density between 35 and 48 kg/m^3. The average densities of CO-RPUF with DMMP, TEP, MC, and EG were 39.90, 42.18, and 42.68 kg/m^3, respectively. This indicated that the incorporation of FRs into HSO-

RPUF changed its apparent density, and the change was more pronounced in the presence of DMMP and TEP. HSO-RPUFs with liquid FRs (DMMP and TEP) showed increased apparent density values with increasing FR amounts [49]. Meanwhile, HSO-RPUFs with solid FR (EG) showed minor fluctuations in the measured concentration range. This might be because the integration of solid FRs makes foaming more complex than that with liquid FRs [50].

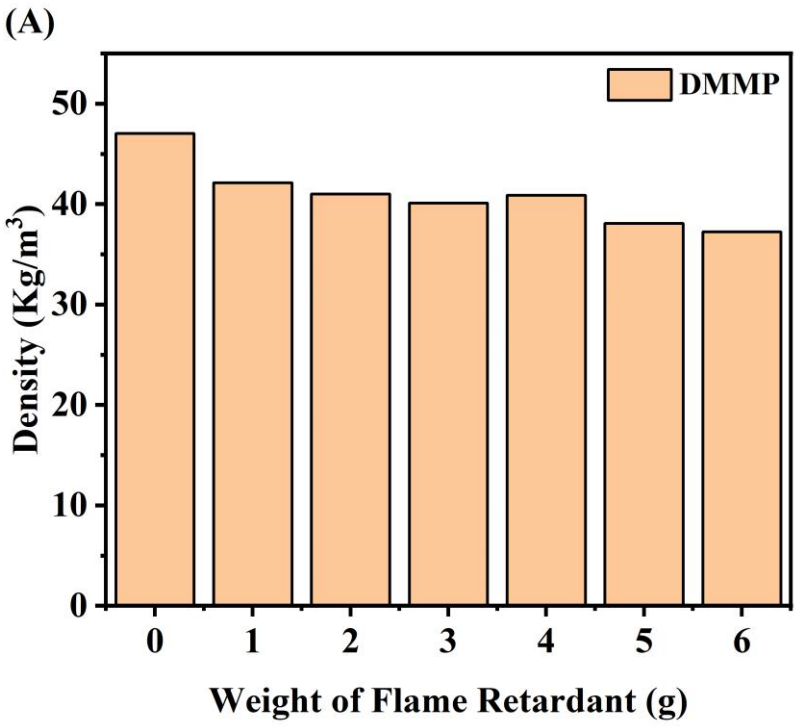

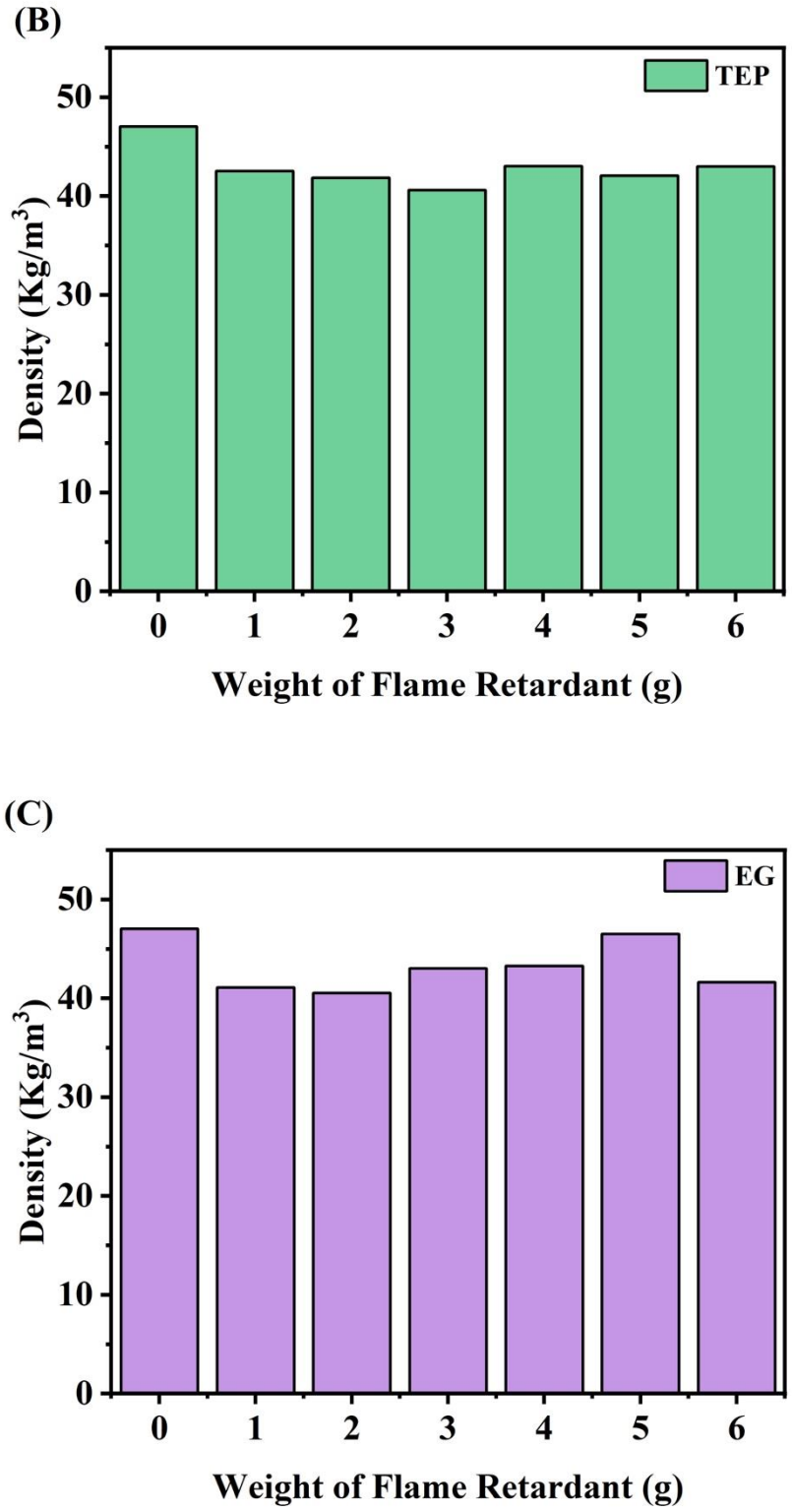

Figure 22. Density for HSO- RPUFs having different amounts of FRs (A) DMMP, (B) TEP, and (C) EG.

3.3.2 Closed Cell Content (CCC)

The CCC of RPUF has a direct impact on its air/moisture permeability, thermal conductivity, and load-bearing capacity. Increased closed cell count leads to higher insulation and reduced heat conductivity. The CCC of RPUFs may be affected by the inclusion of FR, but the extent of this effect has yet to be adequately studied. The closed-cell content of the control HSO-RPUF was 92%. HSO-RPUFs with increasing amounts of DMMP, TEP, and EG maintained closed-cell structures of over 90% without affecting the CCC. The CCC results suggest that adding DMMP, TEP, and EG to RPUFs improves thermal insulation in rigid polyurethane foams [51].

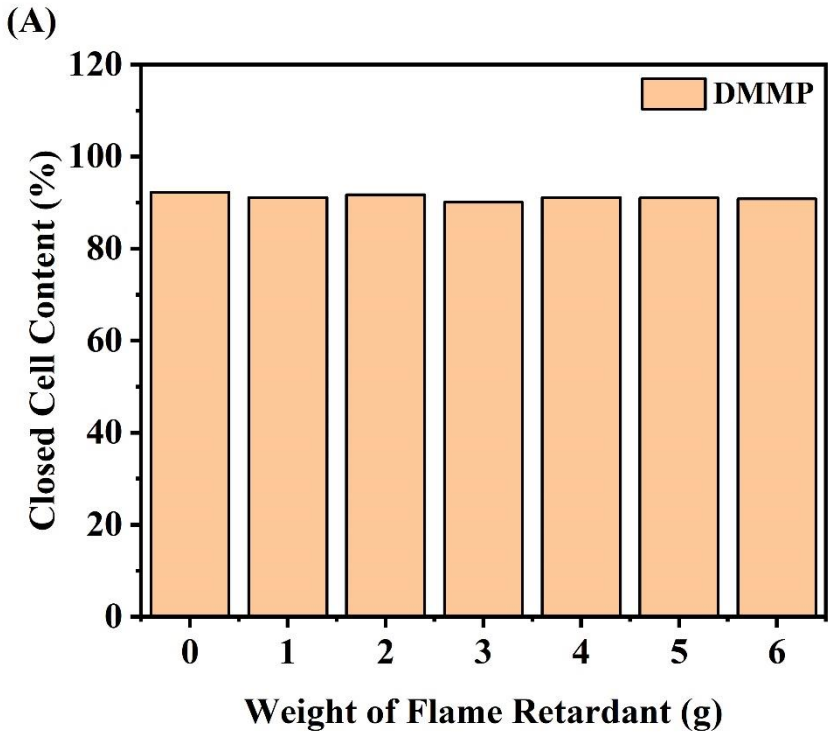

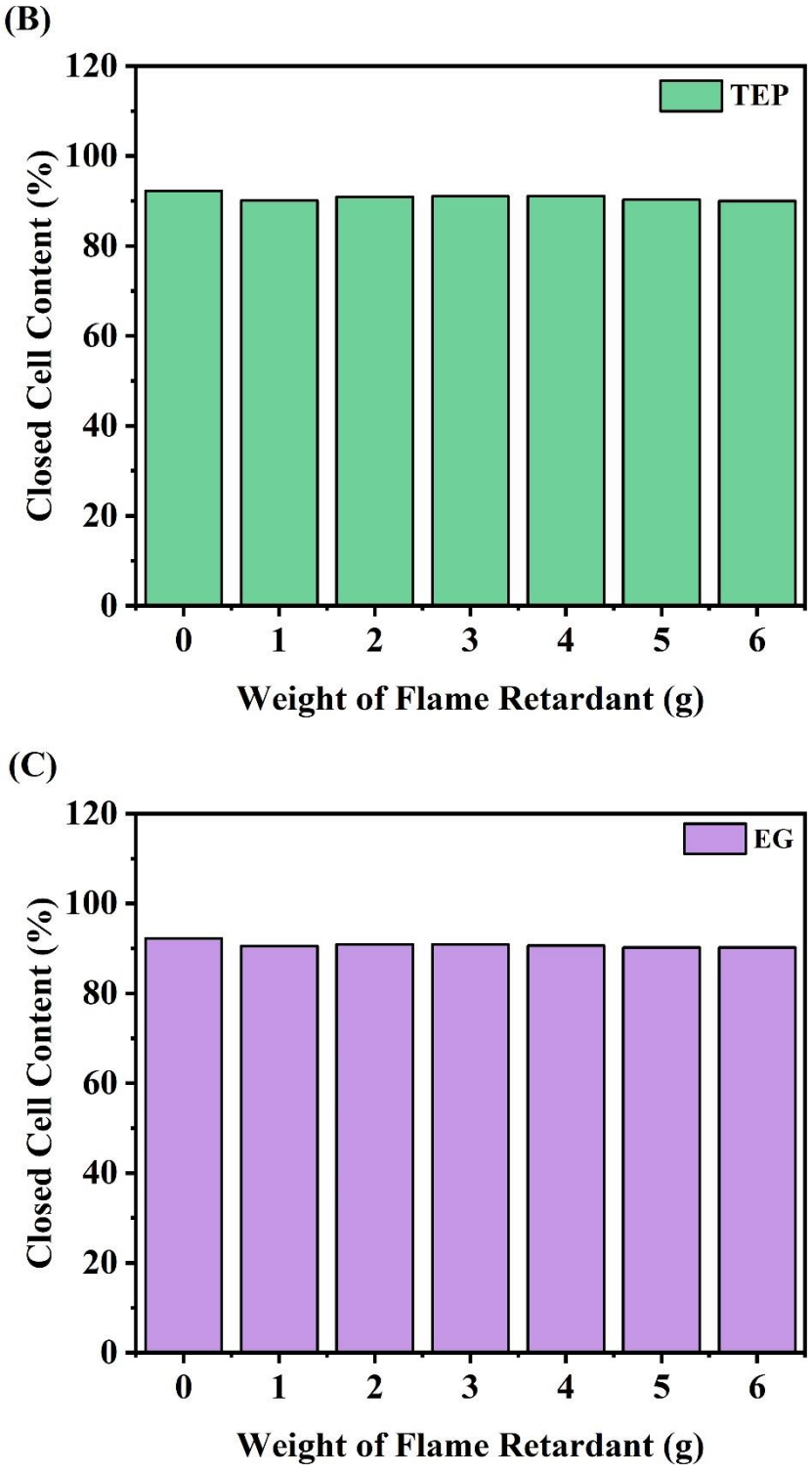

Figure 23. CCC for HSO- RPUFs with different amounts of FRs (A) DMMP, (B) TEP, and (C) EG.

3.3.3. Compression Strength Test

The compression strength of hemp seed oil-based rigid polyurethane foams were evaluated at varying flame-retardant levels (DMMP, TEP, and EG). The analysis examined the yield strength to compare the effects of different flame retardants on foam recovery after compression [52]. This figure was typically observed with a 10% strain or compression. The compressive strength of the rigid polyurethane foams is an important factor for evaluating their mechanical characteristics [53]. The control sample exhibited a yield strength of 257 kN/m^2 at 10% deformation. Meanwhile, the compressive strength decreased to 254 kN/m^2 and 240 kN/m^2 after adding 10.61 wt.% of DMMP-6 and TEP-6, respectively. The observation is likely a result of the plasticizing impact of phosphorous-based flame retardants on the foam, causing a decline in mechanical characteristics. The compressive strength values of the 10.61 wt.% EG-6 was lower at 248 kN/m^2 as compared to the control sample. Moreover, the SEM pictures showed that higher concentrations of DMMP, TEP, and EG led to an enlargement of cell size and a partial disruption of cellular structure [54]. The decrease in the number of cells in the foams was also expected to reduce compressive strength.

(A)

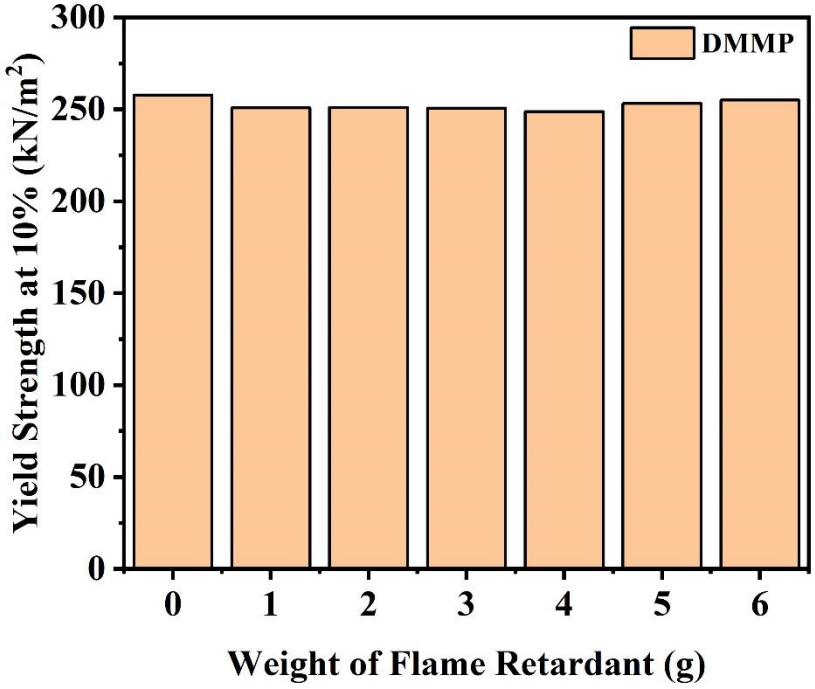
DMMP
Yield Strength at 10% (kN/m²)
300
250
200
150
100
50
0
0
1
2
3
4
5
6
Weight of Flame Retardant (g)

(B)

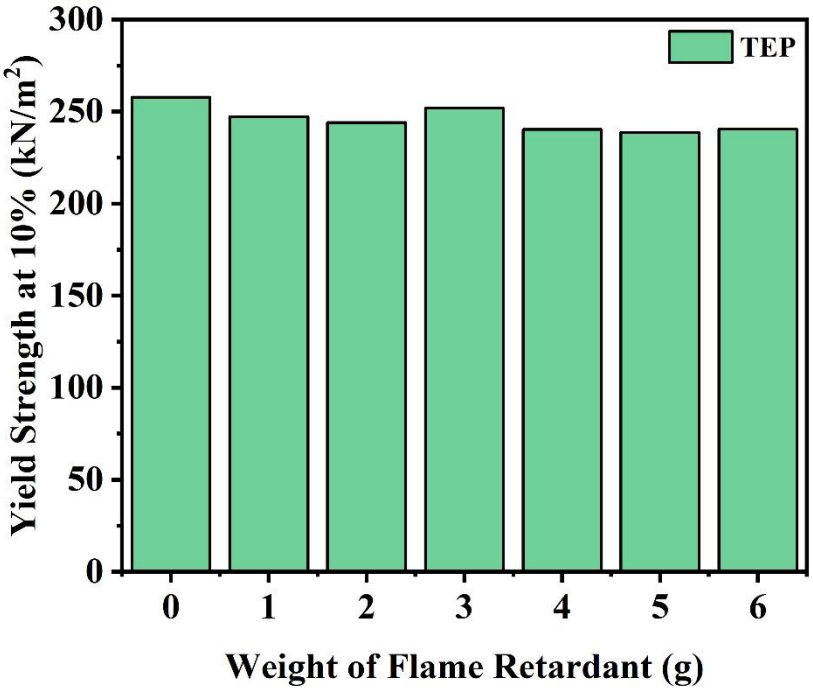
TEP
Yield Strength at 10% (kN/m²)
300
250
200
150
100
50
0
0
1
2
3
4
5
6
Weight of Flame Retardant (g)

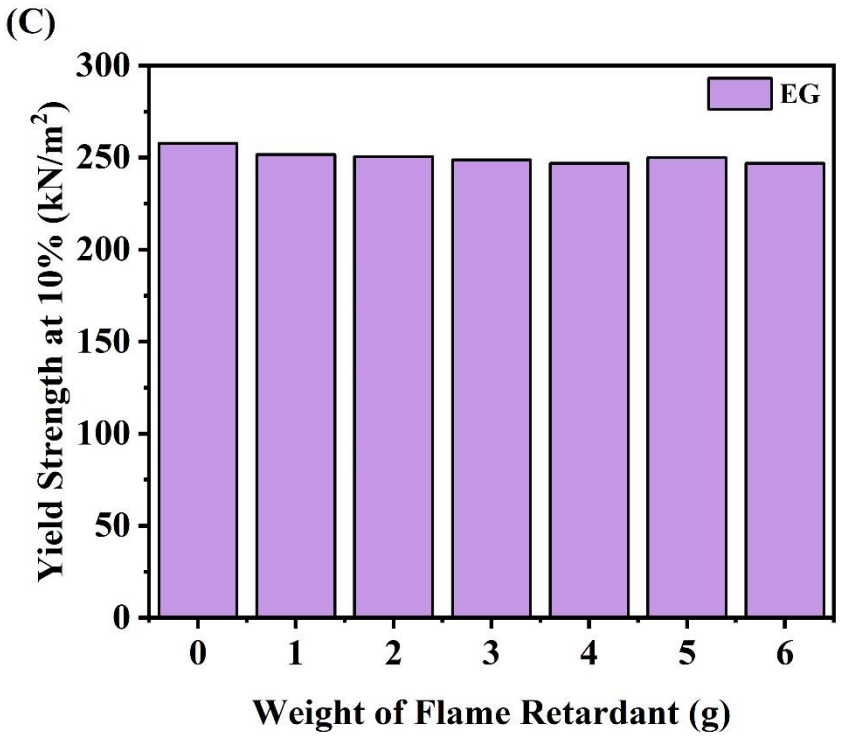

Figure 24. Compression strength for HSO- RPUFs having different amounts of FRs (A) DMMP, (B) TEP, and (C) EG.

3.3.4. Scanning Electron Microscope (SEM)

The impact of various FRs on the shapes and cellular composition of the PUR foams was investigated through scanning electron microscopy **(Figure 25)**. The control sample has an average pore size of 180-250 μm. As the concentration of DMMP increased, the size of the foam cells in DMMP-containing foams also increased progressively. The mean cellular dimensions were computed to be approximately 170-200 μm (**Figure 26A)**. Thus, the enlargement of the cell size balances the above-described reduction in density. Similarly, in the case of TEP and EG-based RPUFs, the cell morphology exhibited a consistently uniform spherical shape at lower loadings.

Nevertheless, as the concentrations are larger, the size of the foam cells rises, and the cellular architecture becomes non-uniform for both TEP and EG-incorporated RPUFs **(Figure 26B)**. The TEP-based RPUFs exhibited an average cell size range from 175-220 μm, whereas the EG-containing foams showed pore diameters of roughly 191-303 μm **(Figure 26C)**. An increase in pore size can be attributed to the collapse of cells, which relates to a small rise in the density of the foams containing EG at higher loadings [55]. The observation indicates a favorable synergy between the FRs and the HSO-based polyurethane matrix [56].

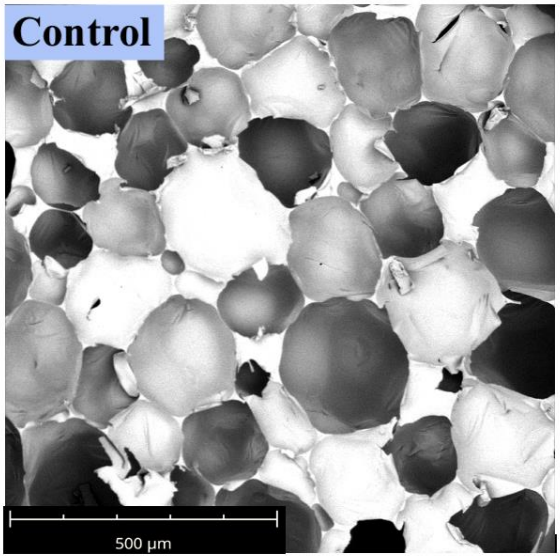

Figure 25. SEM images of HSO-RPUF without FRs

(A)

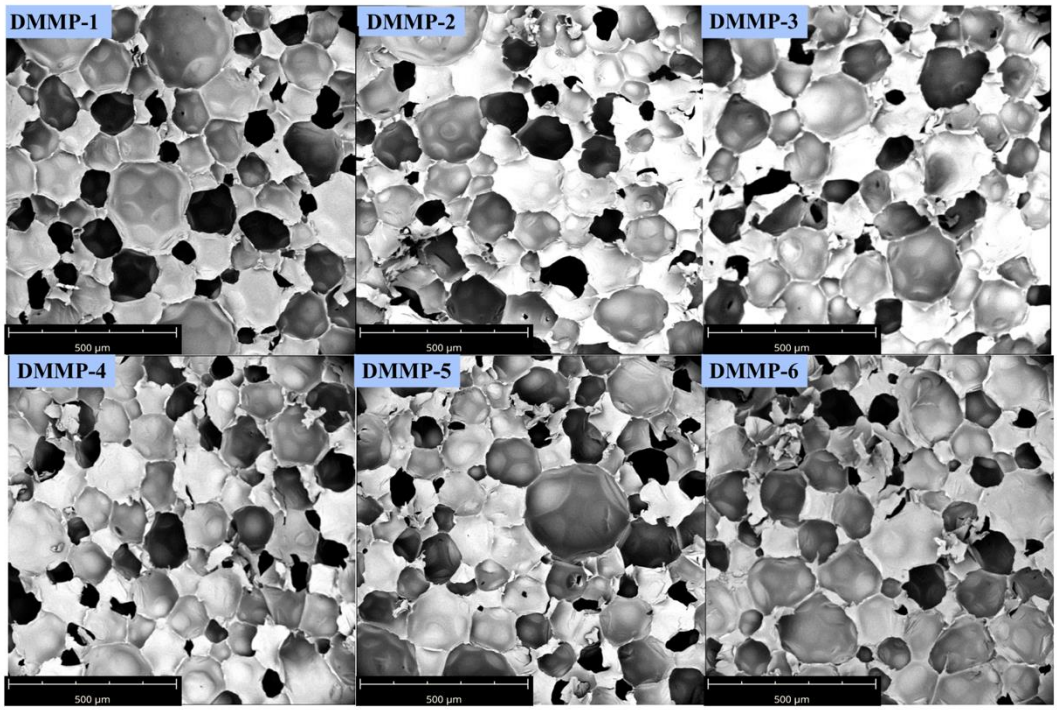
DMMP-1
DMMP-2
DMMP-3
DMMP-4
DMMP-5
DMMP-6
500 µm

(B)

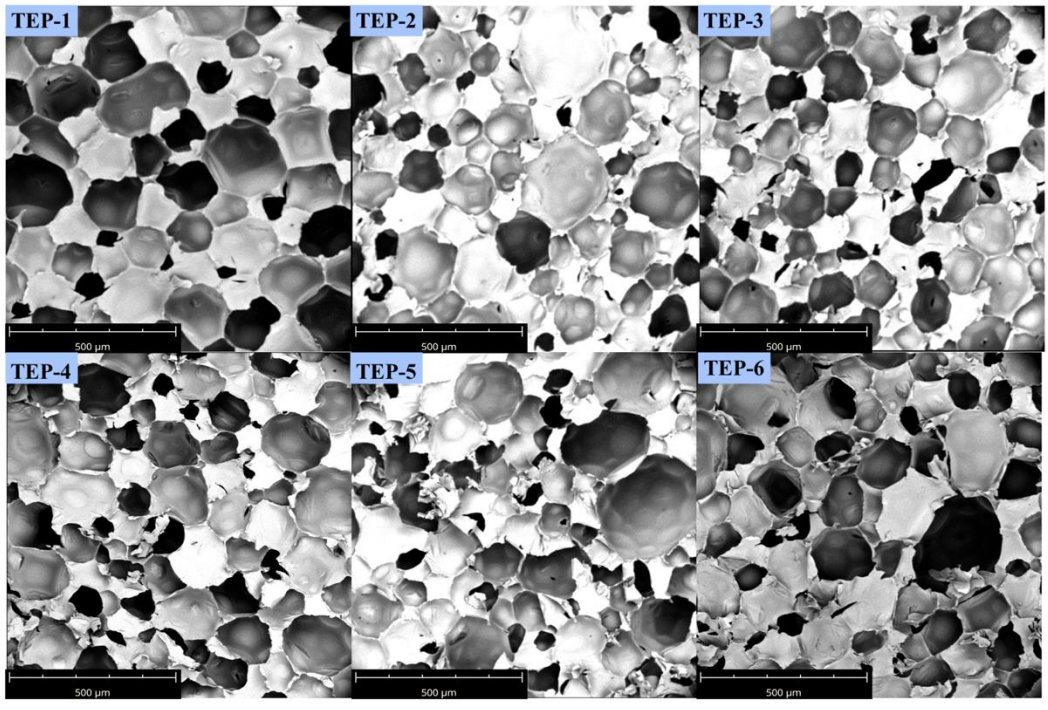
TEP-1
TEP-2
TEP-3
TEP-4
TEP-5
TEP-6
500 µm

(C)

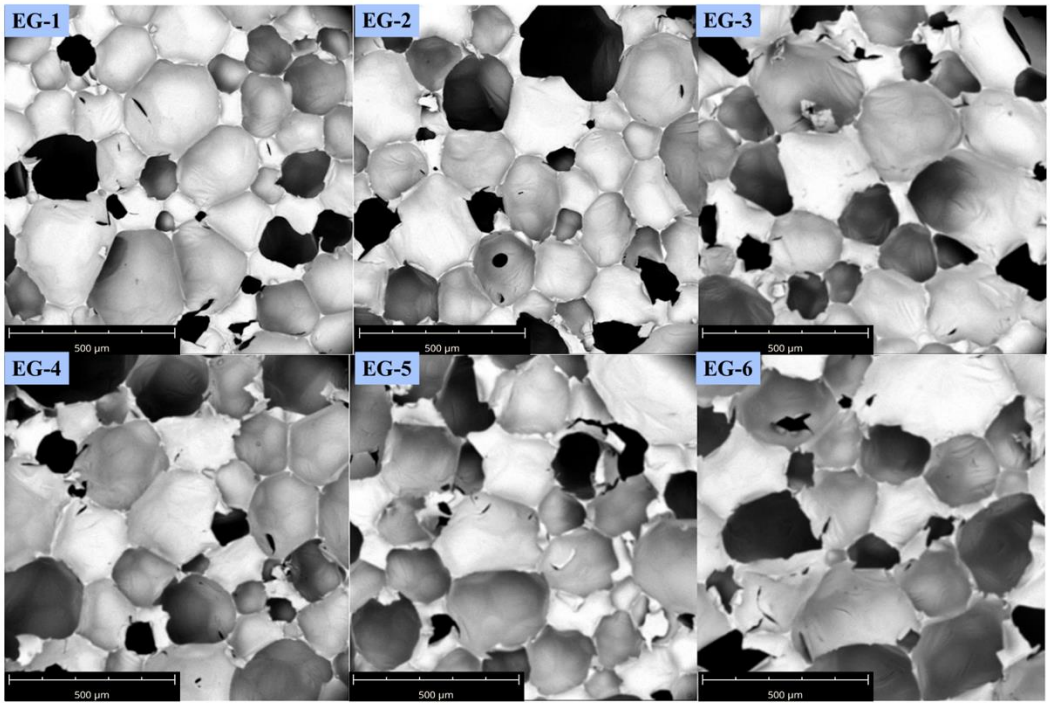

Figure 26. SEM images of HSO-RPUFs with different amounts of FRs (A) DMMP, (B) TEP, and (C) EG.

3.3.5. Horizontal Burning Test

The fire behavior and thermal stability of the rig polyurethane foams were two critical factors in this research [57]. The fire behavior of the HSO-RPUFs was determined using a horizontal burning test. These data are valuable for forecasting fire propagation parameters in the polymer matrix and assessing the combustion stability of the HSO-RPUFs. The experiment showed the burning time and weight loss percentage and measured the surface flame spread after igniting. Excessive burning can cause significant structural damage to the polymeric foam matrix and harm humans extensively, as well as the emission of toxic gasses. Therefore, the goal was to reduce the burning time and increase the thermal stability of HSO-RPUFs [55].

The specimen of HSO-RPUFs without FRs (Control sample) ignited for 104 sec and showed a more significant difference than before burning, which lost up to 81.57% of its initial weight. When comparing all the samples, the burning times and percentage weight loss showed a progressive reduction compared to the control. The samples that had the highest levels of FR demonstrated the most positive results. [58,59]. Curiously, the duration of self-extinguishing in the HSO-RPUFs containing more than 10.61 wt.% percent of DMMP and TEP was less than 15 seconds, but EG took less than 25 seconds. This suggests that the process of flame retardation in the gas phase had a notable impact during the early stages of igniting. When compared to the other samples, the specimens containing phosphorous-based FRs (DMMP and TEP) exhibited much shorter burning periods, but those containing carbon-based FRs (EG) experienced a substantially lower proportion of weight loss, approximately 4.91%. Nevertheless, the presence of FRs in the polymer matrix can restrict fire spread by creating a shielding layer. Therefore, DMMP and TEP combined to create a condensed carbonized area on the burning surface, while EG built a serpentine protective layer to prevent the spread of flames [60].

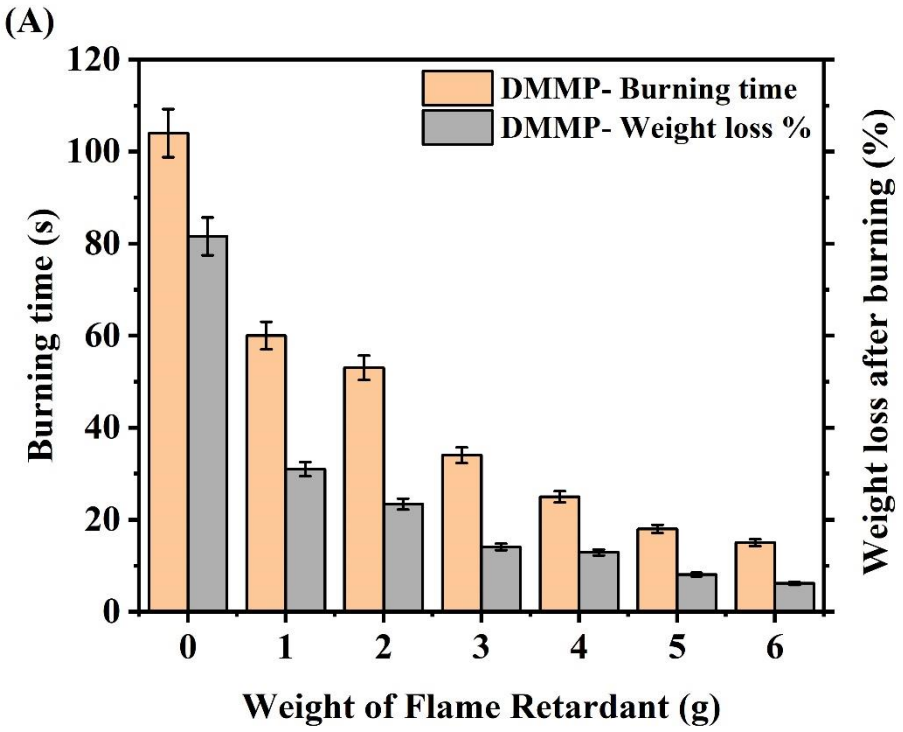
(A)
DMMP- Burning time
DMMP- Weight loss %
Burning time (s)
Weight loss after burning (%)
Weight of Flame Retardant (g)
0
20
40
60
80
100
120
0
1
2
3
4
5
6

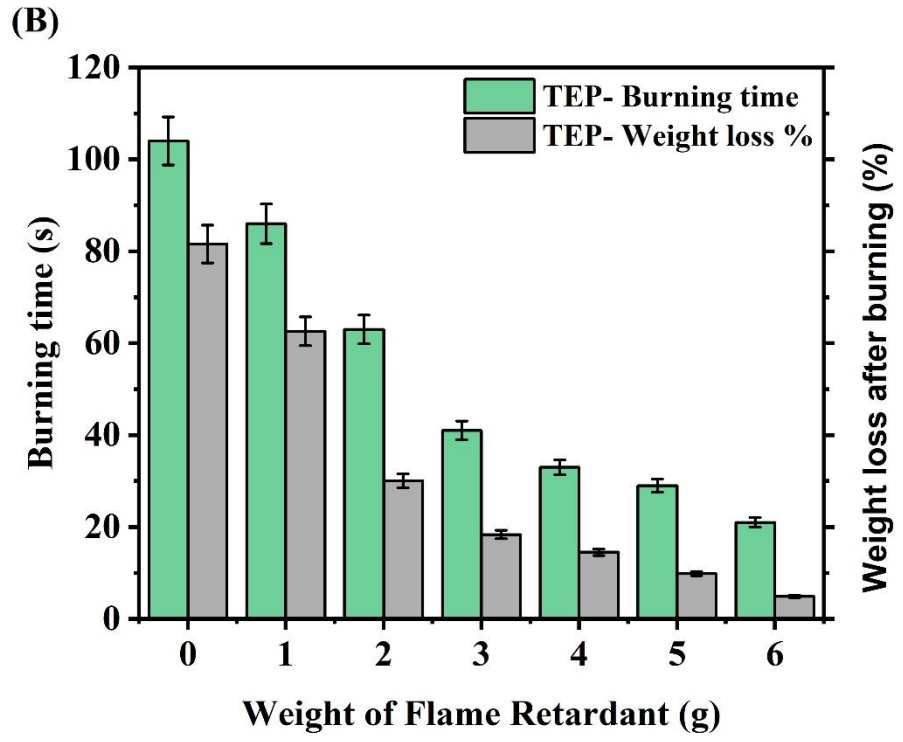
(B)
TEP- Burning time
TEP- Weight loss %
Burning time (s)
Weight loss after burning (%)
Weight of Flame Retardant (g)
0
20
40
60
80
100
120
0
1
2
3
4
5
6

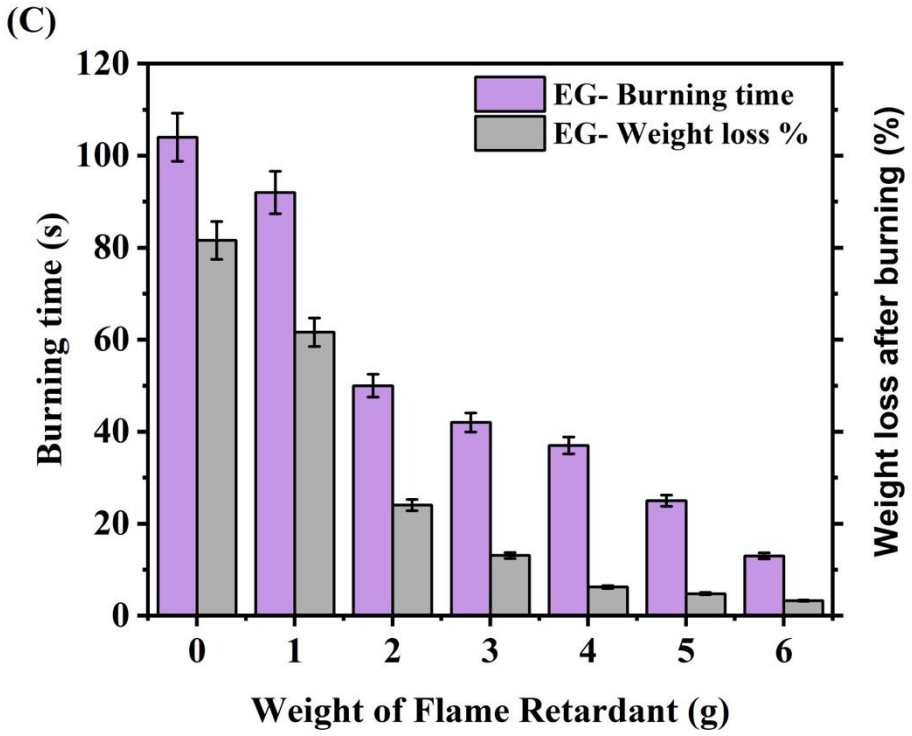

Figure 27. Burning time and weight loss % of HSO-RPUFs with different amounts of FRs (A) DMMP, (B) TEP, and (C) EG.

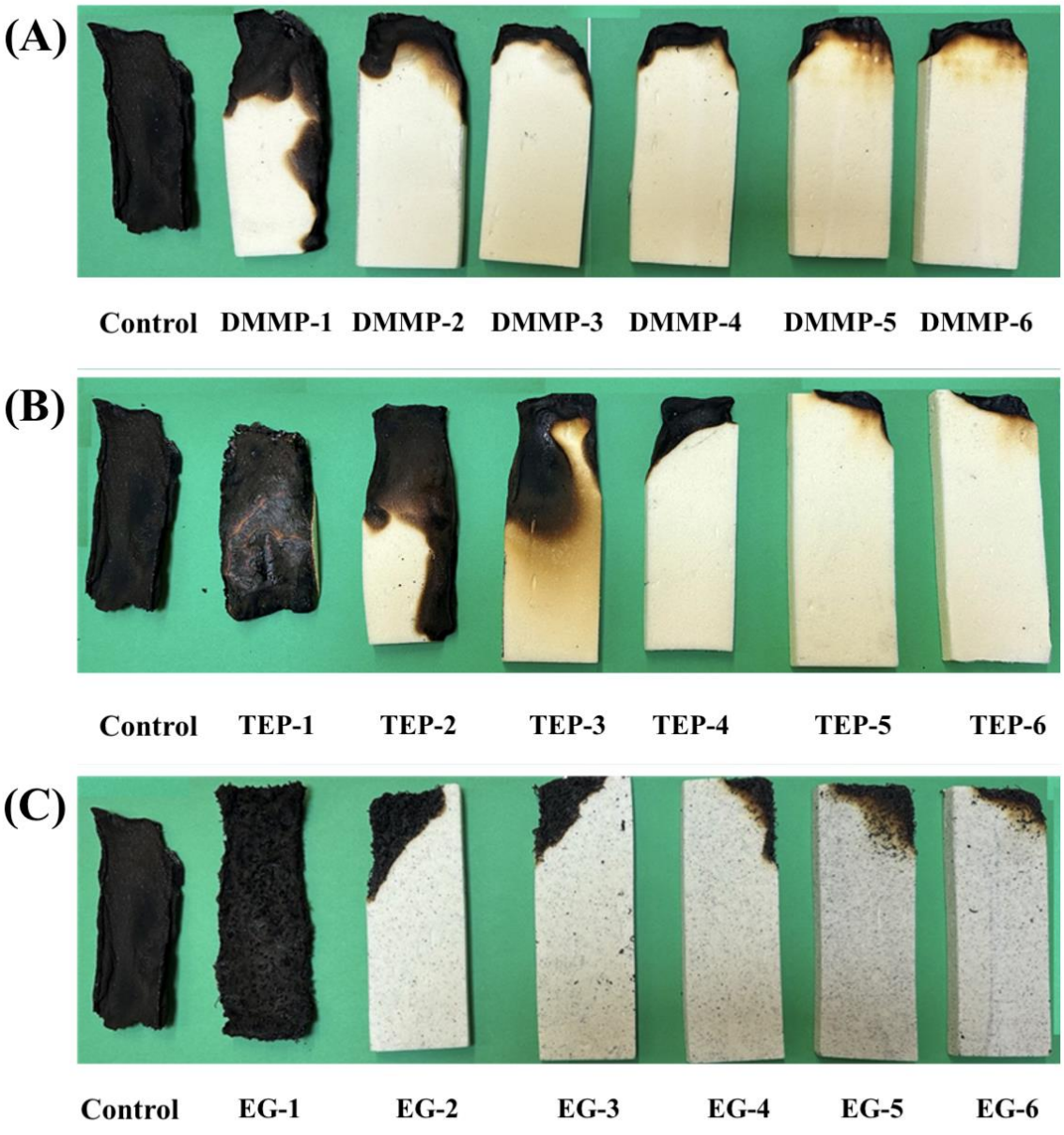

Figure 28. Digital photos of the HSO-RPUFs after the horizontal burning test, (A) DMMP, (B) TEP, and (C) EG.

3.3.6. TGA and DTGA

To understand the thermal stability of the HSO-RPUFs, TGA and derivative thermogravimetric analysis (DTGA) were conducted. **Figure 29-31** shows the TGA and DTGA plots for the foams containing flame retardants[61]. The near RPUF sample shows the two-step degradation stages. The first stage of degradation occurs between 200 to 350 °C for hard segments such as urethane linkage, and the second stage of degradation was observed from 350 °C to 450 °C for thermal breakdown [62][63]. Meanwhile, the P-base containing RPUFs shows the three stages of degradation. The first peak (80°C- 200 °C) shows the vaporization and breakdown of FRs (DMMP and TEP). The second weight loss, occurring between 200°C and 350 °C, is caused by the breakdown of the urethane linkage, which is followed by a breakdown of the polyol and isocyanate at over 370 °C. Significantly, foams with higher concentrations (10.61 wt.%) of FRs (DMMP-6 and TEP-6) exhibited less weight loss compared to the pure foam, suggesting enhanced thermal stability. Foams containing a greater amount of DMMP and TEP have a higher residual char yield, exceeding 13 wt.%, compared to the control sample, which yields 10 wt.% of char residues.

However, HSO-based RPUF foams combined with carbon-based flame retardants (EG) showed a two-step thermal breakdown mechanism, as shown in **Figure 31**. In this result, the initial breakdown was observed from 250 to 350 °C. This breakdown can be attributed to the thermal cleavage of the hard sections and the urethane bond, as mentioned earlier. The second decomposition was linked to the subsequent degradation of isocyanate and polyol as a soft segment. Furthermore, the irreversible shedding of EG leads to releasing CO_2, SO_2, and H_2O gases at temperatures ranging from 250 to 300 °C.

In addition, the foams with higher concentrations of EG exhibited a greater residue (over 20% by weight) compared to the pure foam. This could be attributed to forming a carbonaceous insulating char layer, like worms, which hinders the total degradation of the material. The results demonstrate that the thermal stability of foams significantly increases when DMMP, TEP, and EG-based flame retardants are added to the polyurethane formulation. Furthermore, the TGA results aligned with the residual weight loss percentage obtained from the flammability tests, suggesting an enhancement in the overall thermal stability following the presence of FRs [63][64].

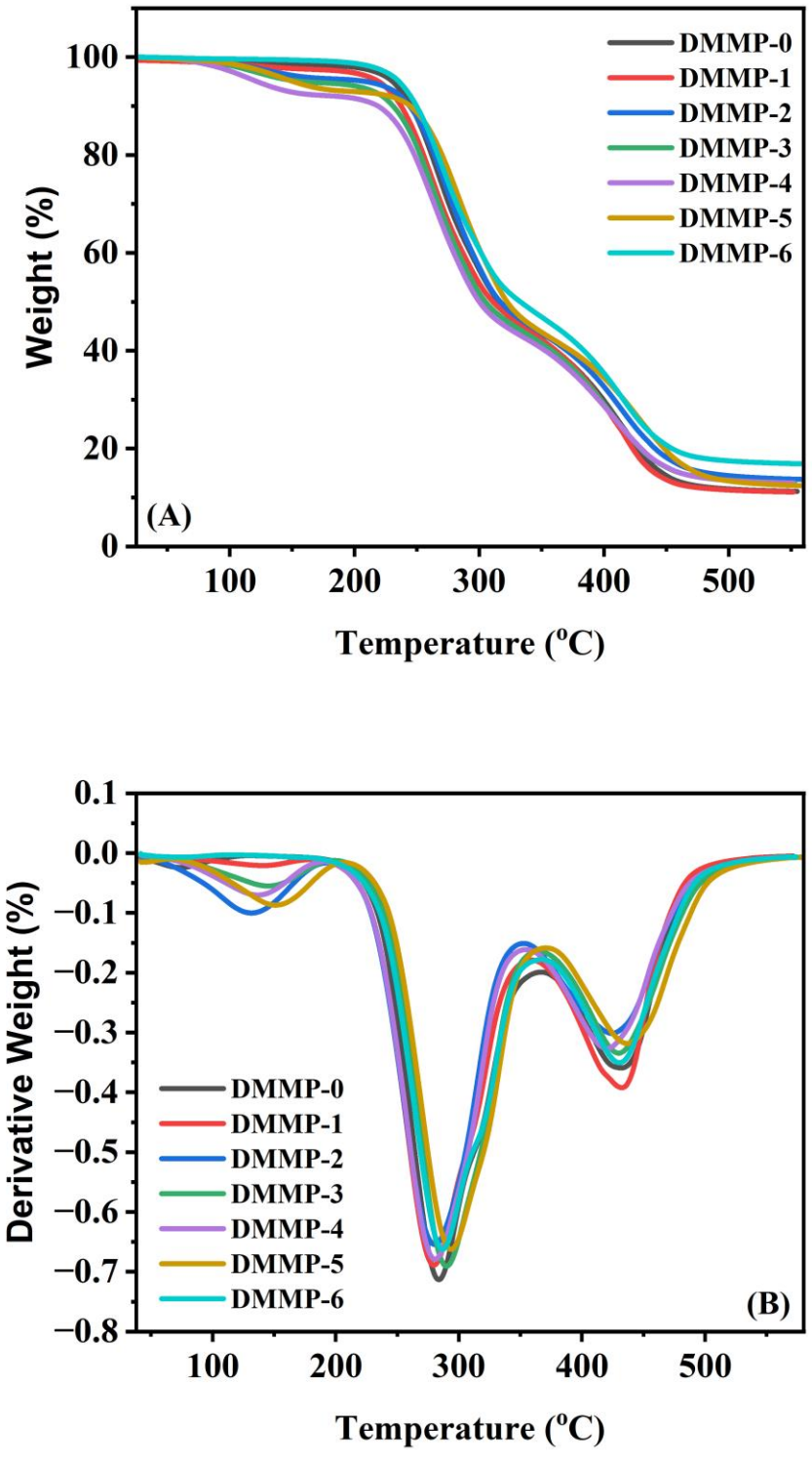

Figure 29. (A) TGA, and (B) DTGA plots of HSO-RPUFs with different amounts of DMMP.

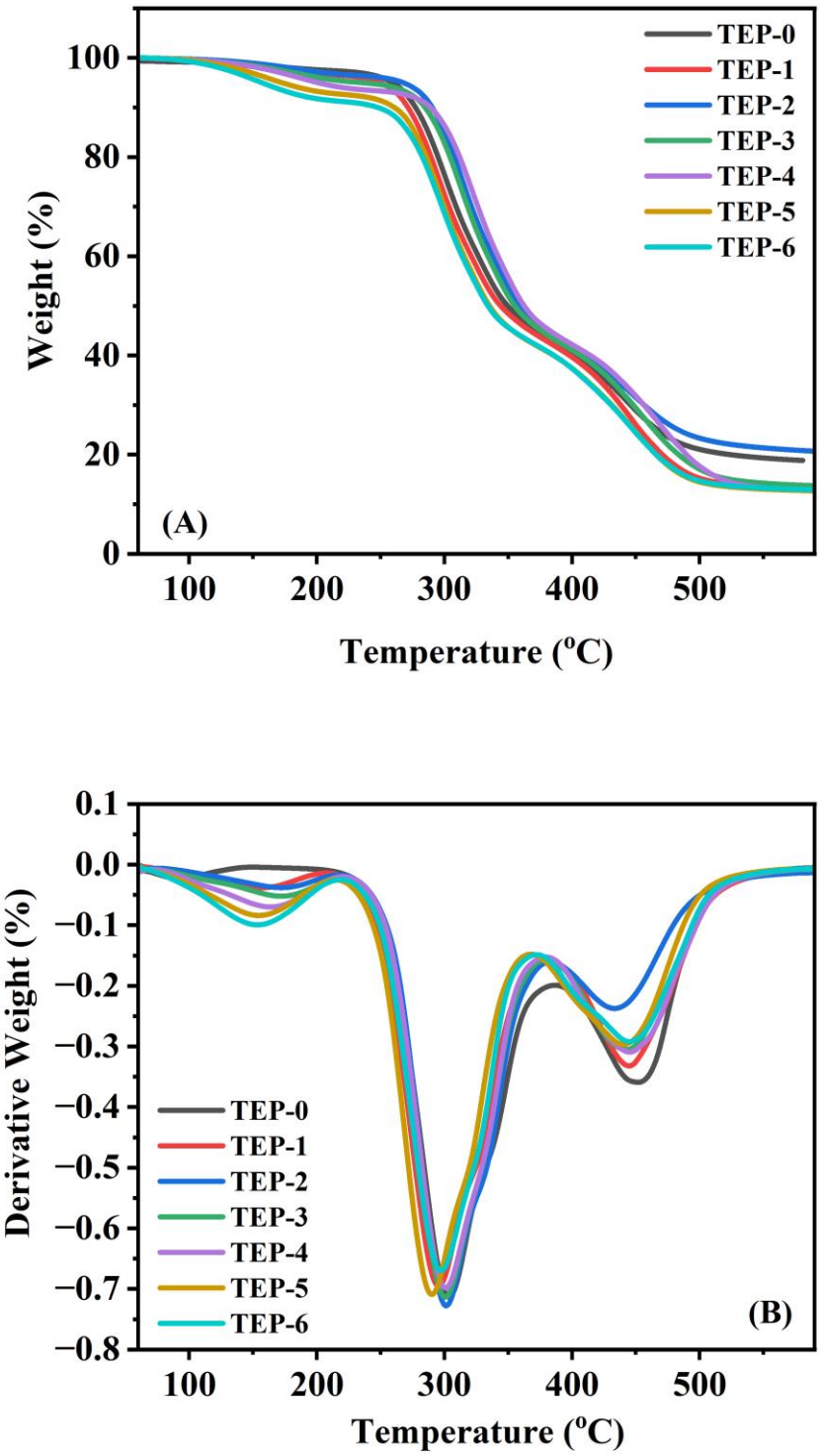

Figure 30. (A) TGA, and (B) DTGA plots of HSO-RPUFs with different amounts of TEP.

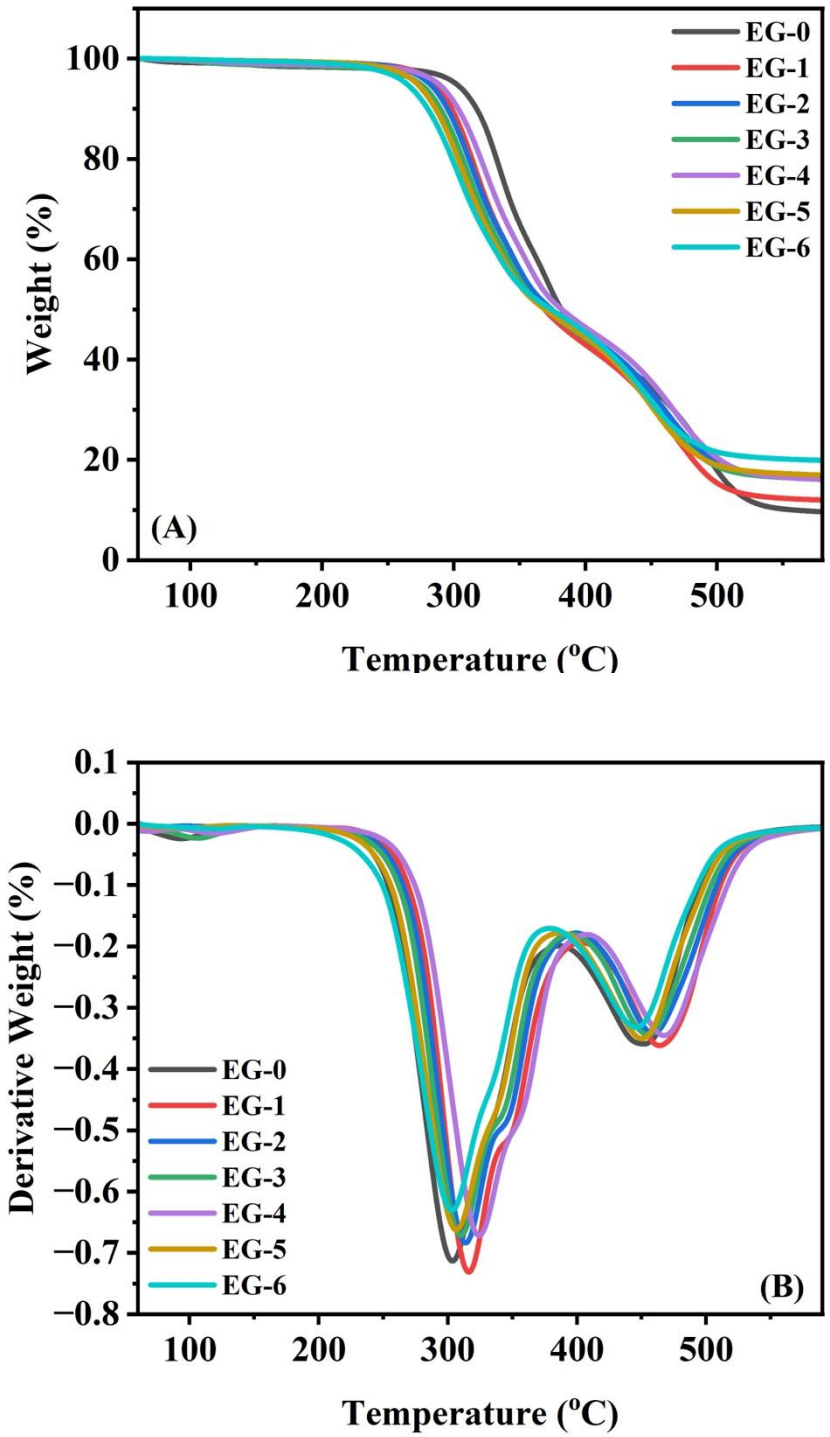

Figure 31. (A) TGA, and (B) DTGA plots of HSO-RPUFs with different amounts of EG.

CHAPTER IV

CONCLUSION

This study investigated the possibility of converting hemp seed oil into highly active bio-based polyols using the epoxidation-oxirane ring-opening method for producing RPUF. As a result, the hydroxyl number of the prepared HSO-polyol was 209 mg KOH/g. Furthermore, the polyol's acid value, viscosity, and specific gravity characteristics confirm its suitability for the commercial manufacture of rigid polyurethane foams. Therefore, RPUF can be manufactured using polyols derived from biological sources. Additionally, the cost of the product can be reduced by using low-cost HSOP. This is because HSOP can be effectively combined with readily accessible biobased polyols.

The HSO-RPUF showed an apparent density of 42.68 kg/m^3, a CCC efficiency of 92%, and a compression strength of 247 kPa. Nevertheless, the HSO-RPUF without FR combusted in just 104 seconds and experienced a significant reduction of 81.57% in its original weight. Therefore, environmentally friendly FRs such as DMMP, TEP, and EG were added to the HSO-RPUF matrix using an additive approach to decrease flammability. The flame retardancy and thermal stability level positively correlated with the percentage of FRs present in HSO-RPUFs. The carbon-based FRs (EG) make HSO-RPUFs more effective in horizontal burning tests than DMMP and TEP. Nevertheless, the

HSO-RPUFs with DMMP and TEP exhibited similar thermal stability results from the condensed and intumescent flame-retardant mechanisms.

Significantly, it was observed that additive FRs, DMMP, TEP, and EG could provide better dispersion in the HSO-PRUF matrix without damaging its pristine chemical structure. The main criteria for RPUF are its low weight, dense closed-cell structure, and outstanding load-bearing capacity. HSO-RPUFs containing DMMP, and TEP had a low density and high Critical CCC but showed relatively low compression strength. HSO-RPUFs with EG exhibited superior physiochemical, mechanical, and thermal properties compared to P-based FRs (DMMP and TEP).

FUTURE SUGGESTIONS

The applications of RPUF are experiencing significant growth beyond conventional uses in building insulation, including composites, sandwich panels, etc. Therefore, a sustainable alternative to petroleum-based raw materials should be developed. Further research should be conducted to identify novel bio-based materials and formulations. For instance, the developing sources of polyols that have been verified in laboratory experiments include jatropha oil, chicken fat, corn, peanuts, and cottonseed oil. Further research is required to establish a correlation between the chemistry of these substances and their physical, mechanical, and thermal properties. Additional investigation is necessary to ascertain the safety and efficacy of different flame retardants for various applications.

REFERENCES

[1] C. Zhang, R. Ding, M.R. Kessler, Reduction of epoxidized vegetable oils: A novel method to prepare bio-based polyols for polyurethanes, Macromol Rapid Commun. 35 (2014) 1068–1074.

[2] M.A. Asare, F.M. De Souza, R.K. Gupta, Waste to Resource: Synthesis of Polyurethanes from Waste Cooking Oil, Ind Eng Chem Res. 61 (2022) 18400–18411.

[3] R. Kaur, P. Singh, S. Tanwar, G. Varshney, S. Yadav, Assessment of Bio-Based Polyurethanes: Perspective on Applications and Bio-Degradation, Macromol. 2 (2022).

[4] A. Tenorio-Alfonso, M.C. Sánchez, J.M. Franco, A Review of the Sustainable Approaches in the Production of Bio-based Polyurethanes and Their Applications in the Adhesive Field, J Polym Environ. 28 (2020) 749–774.

[5] E.R. Ghomi, F. Khosravi, Z. Mossayebi, A.S. Ardahaei, F.M. Dehaghi, M. Khorasani, R.E. Neisiany, O. Das, A. Marani, R.A. Mensah, L. Jiang, Q. Xu, M. Försth, F. Berto, S. Ramakrishna, The Flame Retardancy of Polyethylene Composites: From Fundamental Concepts to Nanocomposites, Molecules. 25 (2020).

[6] S. Khanal, Y. Lu, S. Ahmed, M. Ali, S. Xu, Synergistic effect of zeolite 4A on thermal, mechanical and flame retardant properties of intumescent flame retardant HDPE composites, Polym Test. 81 (2020) 106177.

[7] K. Salasinska, K. Mizera, M. Celiński, P. Kozikowski, M. Borucka, A. Gajek, Thermal properties and fire behavior of polyethylene with a mixture of copper

phosphate and melamine phosphate as a novel flame retardant, Fire Saf J. 115 (2020).

[8] O. Das, R.E. Neisiany, A.J. Capezza, M.S. Hedenqvist, M. Försth, Q. Xu, L. Jiang, D. Ji, S. Ramakrishna, The need for fully bio-based facemasks to counter coronavirus outbreaks: A perspective, Science of the Total Environment. 736 (2020) 139611.

[9] J. Peyrton, L. Avérous, Structure-properties relationships of cellular materials from biobased polyurethane foams, Materials Science and Engineering R: Reports. 145 (2021).

[10] Y. Kim, S. Lee, H. Yoon, Fire-Safe polymer composites: Flame-retardant effect of nanofillers, Polymers (Basel). 13 (2021) 1–49.

[11] D.K. Chattopadhyay, D.C. Webster, Thermal stability and flame retardancy of polyurethanes, Progress in Polymer Science (Oxford). 34 (2009) 1068–1133.

[12] M.L. Pinto, Formulation, preparation, and characterization of polyurethane foams, J Chem Educ. 87 (2010) 212–215.

[13] A. Das, P. Mahanwar, A brief discussion on advances in polyurethane applications, Advanced Industrial and Engineering Polymer Research. 3 (2020) 93–101.

[14] R. Kaur, P. Singh, S. Tanwar, G. Varshney, S. Yadav, Assessment of Bio-Based Polyurethanes: Perspective on Applications and Bio-Degradation, Macromol. 2 (2022) 284–314.

[15] H.W. Engels, H.G. Pirkl, R. Albers, R.W. Albach, J. Krause, A. Hoffmann, H. Casselmann, J. Dormish, Polyurethanes: Versatile materials and sustainable

problem solvers for today's challenges, Angewandte Chemie - International Edition. 52 (2013) 9422–9441.

[16] M.A. Sawpan, Polyurethanes from vegetable oils and applications: a review, Journal of Polymer Research. 25 (2018).

[17] J. Brzeska, A. Piotrowska-Kirschling, A brief introduction to the polyurethanes according to the principles of green chemistry, Processes. 9 (2021).

[18] P. Furtwengler, L. Avérous, Renewable polyols for advanced polyurethane foams from diverse biomass resources, Polym Chem. 9 (2018) 4258–4287.

[19] D. Kyriacos, Biobased polyols for industrial polymers, 2020.

[20] Y.Y. Li, X. Luo, S. Hu, Bio-based Polyols and Polyurethanes, Bio-Based Polyols and Polyurethanes. (2015) 1–79.

[21] M. Desroches, M. Escouvois, R. Auvergne, S. Caillol, B. Boutevin, From vegetable oils to polyurethanes: Synthetic routes to polyols and main industrial products, Polymer Reviews. 52 (2012) 38–79.

[22] H. Sardon, D. Mecerreyes, A. Basterretxea, L. Avérous, C. Jehanno, From Lab to Market: Current Strategies for the Production of Biobased Polyols, ACS Sustain Chem Eng. 9 (2021) 10664–10677.

[23] B.D. Oomah, M. Busson, D. V. Godfrey, J.C.G. Drover, Characteristics of hemp (Cannabis sativa L.) seed oil, Food Chem. 76 (2002) 33–43.

[24] J. Liang, A. Appukuttan Aachary, U.T. Hollader, Hemp seed oil: Minor components and oil quality, Lipid Technol. 27 (2015) 231–233.

[25] V. Mikulcová, V. Kašpárková, P. Humpolíček, L. Buňková, Formulation, characterization and properties of hemp seed oil and its emulsions, Molecules. 22 (2017) 1–13.

[26] L. Quiles-Carrillo, M.M. Blanes-Martínez, N. Montanes, O. Fenollar, S. Torres-Giner, R. Balart, Reactive toughening of injection-molded polylactide pieces using maleinized hemp seed oil, Eur Polym J. 98 (2018) 402–410.

[27] Document downloaded from : This paper must be cited as : Quiles-Carrillo , L .; Blanes-Martínez , M .; Montanes , N .; Fenollar , O .; Torres-Giner , S .; Balart , R . (2018). Reactive toughening of injection-molded polylactide pieces using maleinized T, (2018) 402–410.

[28] A. Yadav, F.M. De Souza, T. Dawsey, R.K. Gupta, Recent Advancements in Flame-Retardant Polyurethane Foams: A Review, Ind Eng Chem Res. 61 (2022) 15046–15065.

[29] F.M. De Souza, Y. Desai, R.K. Gupta, Introduction to Polymeric Foams, ACS Symposium Series. 1439 (2023) 1–23.

[30] G.T.R. Particles, D. Kowalkowska-zedler, M. Barczewski, A. Piasecki, P. Kosmela, K. Sałasi, Fire-Retardant Flexible Foamed Polyurethane (PU) -Based Composites : Armed and Charmed Ground Tire Rubber, (2024) 1–19.

[31] E.D. Weil, S. V. Levchik, Phosphorus Flame Retardants, 2017.

[32] Y. Yuan, H. Yang, B. Yu, Y. Shi, W. Wang, L. Song, Y. Hu, Y. Zhang, Phosphorus and Nitrogen-Containing Polyols: Synergistic Effect on the Thermal Property and Flame Retardancy of Rigid Polyurethane Foam Composites, Ind Eng Chem Res. 55 (2016) 10813–10822.

[33] M. Liu, B. Peng, G. Su, M. Fang, Reactive Flame Retardants: Are They Safer Replacements?, Environ Sci Technol. 55 (2021) 14477–14479.

[34] M.A. Asare, F.M. De Souza, R.K. Gupta, Waste to Resource: Synthesis of Polyurethanes from Waste Cooking Oil, Ind Eng Chem Res. 61 (2022) 18400–18411.

[35] A.F. Aguilera, P. Tolvanen, J. Wärnå, S. Leveneur, T. Salmi, Kinetics and reactor modelling of fatty acid epoxidation in the presence of heterogeneous catalyst, Chemical Engineering Journal. 375 (2019) 121936.

[36] M.A. Asare, P. Kote, S. Chaudhary, F.M. de Souza, R.K. Gupta, Sunflower Oil as a Renewable Resource for Polyurethane Foams: Effects of Flame-Retardants, Polymers (Basel). 14 (2022).

[37] A. Freites Aguilera, J. Rahkila, J. Hemming, M. Nurmi, G. Torres, T. Razat, P. Tolvanen, K. Eränen, S. Leveneur, T. Salmi, Epoxidation of Tall Oil Catalyzed by an Ion Exchange Resin under Conventional Heating and Microwave Irradiation, Ind Eng Chem Res. 59 (2020) 10397–10406.

[38] Y. Meng, F. Taddeo, A.F. Aguilera, X. Cai, V. Russo, P. Tolvanen, S. Leveneur, The lord of the chemical rings: Catalytic synthesis of important industrial epoxide compounds, Catalysts. 11 (2021).

[39] M. Kurańska, H. Benes, K. Polaczek, O. Trhlikova, Z. Walterova, A. Prociak, Effect of homogeneous catalysts on ring opening reactions of epoxidized cooking oils, J Clean Prod. 230 (2019) 162–169.

[40] L.F. Mamuye, A.S. Reshad, Reactive Extraction for Fatty Acid Methyl Ester Production from Castor Seeds Using a Heterogeneous Base Catalyst: Process

Parameter Optimization and Characterization, ACS Omega. 7 (2022) 41559–41574.

[41] M.A. Asare, F.M. De Souza, R.K. Gupta, Waste to Resource: Synthesis of Polyurethanes from Waste Cooking Oil, Ind Eng Chem Res. 61 (2022) 18400–18411.

[42] R. Moulian, F. Zheng, G. Salvato Vallverdu, C. Barrere-Mangote, Q. Shi, P. Giusti, B. Bouyssiere, Understanding the Vanadium-Asphaltene Nanoaggregate Link with Silver Triflate Complexation and GPC ICP-MS Analysis, Energy and Fuels. 34 (2020) 13759–13766.

[43] M. Arefmanesh, T. V. Vuong, J.K. Mobley, M. Alinejad, E.R. Master, M. Nejad, Bromide-Based Ionic Liquid Treatment of Hardwood Organosolv Lignin Yielded a More Reactive Biobased Polyol, Ind Eng Chem Res. 59 (2020) 18740–18747.

[44] J. Dísouza, S.Z. Wong, R. Camargo, N. Yan, Solvolytic Liquefaction of Bark: Understanding the Role of Polyhydric Alcohols and Organic Solvents on Polyol Characteristics, ACS Sustain Chem Eng. 4 (2016) 851–861.

[45] D. Ji, Z. Fang, W. He, K. Zhang, Z. Luo, T. Wang, K. Guo, Synthesis of soy-polyols using a continuous microflow system and preparation of soy-based polyurethane rigid foams, ACS Sustain Chem Eng. 3 (2015) 1197–1204.

[46] S. Wang, S. Wang, M. Shen, X. Xu, H. Liu, D. Wang, H. Wang, S. Shang, Biobased Phosphorus Siloxane-Containing Polyurethane Foam with Flame-Retardant and Smoke-Suppressant Performances, ACS Sustain Chem Eng. 9 (2021) 8623–8634.

[47] M.J. Chen, Y.J. Xu, W.H. Rao, J.Q. Huang, X.L. Wang, L. Chen, Y.Z. Wang, Influence of valence and structure of phosphorus-containing melamine salts on the decomposition and fire behaviors of flexible polyurethane foams, Ind Eng Chem Res. 53 (2014) 8773–8783.

[48] J. Liu, Z. Sun, F. Wang, D. Zhu, J. Ge, H. Su, Facile Solvent-Free Preparation of Biobased Rigid Polyurethane Foam from Raw Citric Acid Fermentation Waste, Ind Eng Chem Res. 59 (2020) 10308–10314.

[49] W.F. Gale, T.C. Totemeier, L. Lane, W. Road, P. Erin, Smithells Metal Reference Book , 8th Ed . Thermal Design of Electronic Polymeric Foams :, (2004) 56.

[50] M. Thirumal, D. Khastgir, G.B. Nando, Y.P. Naik, N.K. Singha, Halogen-free flame retardant PUF: Effect of melamine compounds on mechanical, thermal and flame retardant properties, Polym Degrad Stab. 95 (2010) 1138–1145.

[51] A. Kairyte, A. Kremensas, G. Balčiunas, S. Członka, A. Strakowska, Closed cell rigid polyurethane foams based on low functionality polyols: Research of dimensional stability and standardised performance properties, Materials. 13 (2020).

[52] K. Polaczek, M. Kurańska, Hemp Seed Oil and Oilseed Radish Oil as New Sources of Raw Materials for the Synthesis of Bio-Polyols for Open-Cell Polyurethane Foams, Materials. 15 (2022).

[53] S. Bhoyate, M. Ionescu, P.K. Kahol, J. Chen, S.R. Mishra, R.K. Gupta, Highly flame-retardant polyurethane foam based on reactive phosphorus polyol and limonene-based polyol, J Appl Polym Sci. 135 (2018) 16–19.

[54] Y. Yang, H. Feng, Y. Zhang, Y. Wang, M. Ma, P. Zhu, Mechanical Properties and Brittleness Characterization Method of Low-Rank Coal and Its Char Particles under a Uniaxial Compression Test, Energy and Fuels. 37 (2023) 7696–7706.

[55] R. Kaur, M. Kumar, Addition of anti-flaming agents in castor oil based rigid polyurethane foams: Studies on mechanical and flammable behaviour, Mater Res Express. 7 (2020).

[56] H. Choe, Y. Choi, J.H. Kim, Threshold cell diameter for high thermal insulation of water-blown rigid polyurethane foams, Journal of Industrial and Engineering Chemistry. 73 (2019) 344–350.

[57] M. Kurańska, H. Beneš, K. Sałasińska, A. Prociak, E. Malewska, K. Polaczek, Development and characterization of “green open-cell polyurethane foams” with reduced flammability, Materials. 13 (2020) 1–17.

[58] M. Günther, A. Lorenzetti, B. Schartel, Fire phenomena of rigid polyurethane foams, Polymers (Basel). 10 (2018).

[59] M. Günther, S. V. Levchik, B. Schartel, Bubbles and collapses: Fire phenomena of flame-retarded flexible polyurethane foams, Polym Adv Technol. 31 (2020) 2185–2198.

[60] M.M. Velencoso, A. Battig, J.C. Markwart, B. Schartel, F.R. Wurm, Molecular Firefighting—How Modern Phosphorus Chemistry Can Help Solve the Challenge of Flame Retardancy, Angewandte Chemie - International Edition. 57 (2018) 10450–10467.

[61] U. Stirna, I. Beverte, V. Yakushin, U. Cabulis, Mechanical properties of rigid polyurethane foams at room and cryogenic temperatures, Journal of Cellular Plastics. 47 (2011) 337–355.

[62] B. Dittrich, K.A. Wartig, R. Mülhaupt, B. Schartel, Flame-retardancy properties of intumescent ammonium poly(phosphate) and mineral filler magnesium hydroxide in combination with graphene, Polymers (Basel). 6 (2014) 2875–2895.

[63] S. Ramanujam, C. Zequine, S. Bhoyate, B. Neria, P. Kahol, R. Gupta, Novel Biobased Polyol Using Corn Oil for Highly Flame-Retardant Polyurethane Foams, C (Basel). 5 (2019) 13.

[64] P. Acuña, Z. Li, M. Santiago-Calvo, F. Villafañe, M. ángel Rodríguez-Perez, D.Y. Wang, Influence of the characteristics of expandable graphite on the morphology, thermal properties, fire behaviour and compression performance of a rigid polyurethane foam, Polymers (Basel). 11 (2019).